N 62 13979

NASA TN D-1353

NASA TN D-1353

TECHNICAL NOTE

D-1353

FLUTTER OF AERODYNAMICALLY HEATED ALUMINUM-ALLOY AND STAINLESS-STEEL PANELS WITH LENGTH-WIDTH RATIO OF 10 AT MACH NUMBER OF 3.0

By Lawrence D. Guy and Herman L. Bohon

Langley Research Center
Langley Station, Hampton, Va.

NATIONAL AERONAUTICS AND SPACE ADMINISTRATION

WASHINGTON July 1962

NATIONAL AERONAUTICS AND SPACE ADMINISTRATION

TECHNICAL NOTE D-1353

FLUTTER OF AERODYNAMICALLY HEATED ALUMINUM-ALLOY AND STAINLESS-STEEL PANELS WITH LENGTH-WIDTH RATIO OF 10 AT MACH NUMBER OF 3.0

By Lawrence D. Guy and Herman L. Bohon

L
1
5
3
5

SUMMARY

An investigation of the effects of aerodynamic heating on the flutter of multibay external-skin panels has been carried out at a Mach number of 3.0 in the Langley 9- by 6-foot thermal structures tunnel. Both aluminum-alloy and 17-7 PH stainless-steel panels with a length-width ratio of 10 for each bay were tested at dynamic pressures between 1,500 psf and 5,000 psf and at stagnation temperatures up to 660° F. In addition, a few tests were made on the lower vertical stabilizer of the X-15 airplane which has external-skin panels unsupported for a length 10 times the width.

All panels showed flutter boundaries characterized by an increase in panel thickness required to prevent flutter with increasing thermally induced stress prior to buckling. After buckling the panels showed flutter boundaries characterized by a decrease in thickness required to prevent flutter with further increases in thermal stress. The largest thickness required to prevent flutter in the presence of aerodynamic heating occurred at the transition between the flat-panel boundary and the buckled-panel boundary. This peak value (for aluminum-alloy panel) was as much as 60 percent greater than the extrapolated value for an unheated, unloaded panel.

Values of the modified-thickness-ratio flutter parameter for the unstressed panels (obtained by extrapolation) were in fair agreement for the aluminum, steel, and X-15 stabilizer panels. Peak values at transition, however, showed large differences due to apparently minor changes in panel-support construction and/or changes in panel-skin material.

INTRODUCTION

Panel flutter is presently recognized as a critical problem area for supersonic and hypervelocity vehicles as evidenced by the fact that several current airplanes have recently encountered panel flutter in flight at supersonic speeds. (See ref. 1.) In addition, wind-tunnel tests on the full-scale vertical tail of the X-15 airplane have shown certain panels to be susceptible to flutter within the operating range of the airplane. (See refs. 2 and 3.) In particular, panels on the vertical stabilizer with a length-width ratio of 10 were found to be susceptible to flutter at a Mach number of 3.0 under conditions of aerodynamic heating. Because aerodynamic heating can alter panel stiffnesses due to thermal stresses or buckling, the panel flutter characteristics would be expected to be affected directly by such heating. Therefore, an experimental investigation has been conducted in the Langley 9- by 6-foot thermal structures tunnel on multibay skin panels having the same length-width ratio as the side panels on the X-15 vertical stabilizer in order to study their flutter characteristics and to establish the effects of aerodynamic heating on the flutter boundaries. A few tests have also been made on the full-scale vertical stabilizer.

Three series of multibay panels have been investigated. Two series of panels had aluminum-alloy skins and a third series had skins of 17-7 PH stainless steel. For all panels, the lateral-edge supports were designed to provide some rotational restraint and to permit partial thermal expansion. Test results for one set of aluminum-alloy panels, which had somewhat flexible supports at the leading and trailing edges, are reported in reference 4. The second series of aluminum-alloy panels and the steel panels were more nearly fixed against rotation and thermal elongation at the leading and trailing edges; the results of tests of these panels are reported herein.

The present investigation was conducted at a Mach number of 3.0, at various dynamic pressures, and at stagnation temperatures up to 660° F. Tests were made on two- and four-bay panels of both aluminum-alloy and 17-7 PH stainless steel and on the actual full-scale vertical stabilizer of the X-15 airplane. For all panels considered in the present report, the unstiffened skin between supports was considered to act structurally as an independent panel so that each bay had a length-width ratio of 10. Panel-surface temperatures were measured by means of thermocouples, frequencies were measured by inductance-type pickups, and high-speed motion pictures were used to study the flutter modes.

SYMBOLS

E	Young's modulus of elasticity
f	frequency of flutter
l	panel length in direction of flow

M Mach number

p static pressure

p_t total pressure

Δp differential pressure across panel skin, positive when bay pressure is greater than free-stream pressure

q dynamic pressure

L1630

T temperature of panel skin

T_i initial temperature of panel skin

T_t stagnation temperature

ΔT incremental temperature $T - T_i$

ΔT_{cr} critical buckling temperature of panel skin

t time

w unsupported bay width, perpendicular to flow

α coefficient of thermal expansion of material

$\beta = \sqrt{M^2 - 1}$

ϵ_x strain in longitudinal direction

σ_x,σ_y panel midplane stress

τ panel-skin thickness

PANEL DESCRIPTION

All panels used in this investigation were of multibay, skin-stiffener-type construction and had skins of 2024-T3 aluminum alloy and 17-7 PH stainless steel. For each panel the skin was attached by two rows of rivets at the leading and trailing edges and by a single row of rivets to longitudinal channels which formed the ribs; the ribs separated the panels into either two or four bays. The skin covering each individual bay had a length-width ratio of 10.

Aluminum-Skin Panels

Geometrical details of the two- and four-bay aluminum panels designated 2-A and 4-A, respectively, are shown in figures 1(a) and 1(b), and a photograph of a four-bay panel is shown in figure 2. The two- and four-bay panels differed in panel length, depth of the panel-skin supports, and in the edge support attachments because of differences in construction of the test fixtures used for mounting the panels. The nominal panel lengths were 27 inches and 26 inches for the two- and four-bay panels, respectively. (See table I.) Dimensions for the longitudinal channels and Z-section supports at the leading and trailing edges are given in figures 1(a) and 1(b). Steel channels were riveted transversely to the bottom of the longitudinal channels to provide support for mounting the instrumentation. The spacer between the outside ribs and the streamwise-edge support angle shown in figure 1(a) for panels 2-A was omitted in the edge attachment for panels 4-A. (See fig. 1(b).) The edge support angle was attached directly to the test fixture for the two-bay panels but was attached to a steel filler plate for the four-bay panels. A 0.05-inch gap was provided between the streamwise edges and the filler plate to permit some thermal expansion; whereas, the attachment at the leading and trailing edges provided approximately a clamped-end condition. For the two-bay panels, bakelite insulation was provided beneath the skin at the leading and trailing edges but was omitted for the four-bay panels. Skin thicknesses for the two- and four-bay aluminum panels are given in table I.

L
1
6
3
0

Steel-Skin Panels

One panel with two bays and two panels with four bays were fabricated by replacing the aluminum-alloy skin with a 0.020-inch-thick 17-7 PH stainless-steel sheet, so that support construction was the same as shown in figures 1(a) and 1(b). These panels have been designated 2-S and $4\text{-}S_1$ in the table and figures. In addition, a four-bay steel-skin panel, designated $4\text{-}S_2$, was fabricated with a length of 28 inches between rivet rows and is shown in figure 1(c). For panels $4\text{-}S_2$, the Z-sections interfered with the test fixture and were omitted. Instead, the leading and trailing edges were fastened directly to the panel holder but were insulated from it by bakelite strips.

X-15 Stabilizer Panels

Pertinent dimensions and details of the all-movable portions of the lower vertical stabilizer of the X-15 airplane are shown in figure 3. The stabilizer is shown inverted in figure 3(a) to correspond to the manner in which it was mounted for testing in the Langley 9- by 6-foot thermal structures tunnel. (See fig. 4.) The skin of the vertical sides of the stabilizer consists of a sheet of 0.030-inch-thick Inconel X, flush riveted to the main spar, ribs, and trailing bulkhead, and a sheet of 0.037-inch-thick Inconel X between the main spar and leading edge. Five ribs separated the internal volume into four bays. An additional corrugated stiffener sheet was spot-welded to the skin in bays numbered one and four. (See fig. 3(a).) The present investigation is concerned only with that portion of the unstiffened skin panels of the two center bays beyond the main spar, the dimensions of which are shown in figure 3(a). Along the streamwise edges the skin was attached by a double row of rivets to a rib cap; the rib cap was welded to a corrugated angle which, in turn, was welded to the corrugated ribs. (See fig. 3(b).) A double row of rivets attached the skin panels to the main spar and trailing-edge bulkhead. The main spar was the main load-carrying structure and was very stiff, whereas the bulkhead was formed of two corrugated sheets spot-welded together. The stabilizer was mounted in the test section by bolting the main spar to the tunnel floor and was further restrained by steel angle shoes along each side. (See fig. 4.) The shoes were bolted to the tunnel floor but not to the stabilizer.

APPARATUS AND TESTS

All tests were conducted in the Langley 9- by 6-foot thermal structures tunnel, an intermittent blowdown facility exhausting to the atmosphere through a diffuser. This tunnel has a test-section Mach number of 3.0 and the capability of providing stagnation temperatures up to 660° F, so that true flight simulation at an altitude of 30,000 feet can be realized. A more detailed description of the tunnel and its operation is given in reference 4.

Vertical Panel Holder

One test fixture was essentially a two-dimensional airfoil which spanned the tunnel from top to bottom, a distance of 6 feet. The cross section was unsymmetrical and had a sharp leading edge beveled on one side and a plane surface from leading edge to the blunt trailing edge on the other. A recess in the unbeveled side, 29 inches by 30 inches, permitted flush mounting of the test panels. (See fig. 5.) Pneumatically operated doors were installed during the course of the investigation to protect test panels from transient loading during the tunnel start and shutdown. A detailed description of the panel holder and the flow conditions over the surface occupied by the panels is given in reference 4.

Horizontal Panel Holder

This test fixture was designed to provide uniform flow conditions, unaffected by the thick test-section wall boundary layer, for tests of semispan wings and control surfaces. The fixture was modified to allow flutter tests of the two-bay panels. The panels were mounted flush with the flat horizontal surface, which had a hexagonal planform (see fig. 6) and was supported $7\frac{1}{2}$ inches above the tunnel floor. Pressure surveys over the surface occupied by the panels showed that the static-pressure ratio p/p_t varied only ± 0.0019 from the average static-pressure ratio. The well below the test panel was sealed from the tunnel airstream except for a vent door on the underside which was used to control the air pressure in the well. No provision was made for protection of the panels from the tunnel starting loads.

L
1
6
3
0

Test Technique

Severe turbulence resulting from flow separation from the tunnel walls accompanied passage of the normal shock wave during start and shutdown of the tunnel and imposed abnormal loads on the test panels. In some cases this transient loading during the tunnel start damaged the test panels and invalidated the test results. It was also found that aerodynamic heating of the panels during the time required to start the tunnel $\left(\text{approximately } 1\frac{1}{2} \text{ seconds}\right)$ could initiate flutter before the desired test conditions could be established. For a few of the first series of tests in which the vertical panel holder was used, the test panels were protected from starting loads by a boilerplate shield which was released by the firing of explosive bolts after the tunnel had started. Later, the pneumatically operated doors (shown in the open position in fig. 5) were installed in such a manner as to enclose the panels completely and protect them from aerodynamic loading and heating during tunnel start and shutdown. Such methods were impractical for use with the horizontal panel holder. However, a row of small orifices in the test-fixture surface upstream of the panel leading edge permitted film cooling of the skin by injection of water into the boundary layer. This cooling protected the test panels from aerodynamic heating during the tunnel start and until the desired flow conditions were obtained.

Fast, accurate control of the air pressure on the backface of the panel was required because of the sudden drop in test-section static pressure during the tunnel start. This pressure change, which exceeded 10 psi and took place in less than $1\frac{1}{2}$ seconds, was sufficient to deform the panels unless followed closely by the change in pressure in the cavity behind the test panel. Preset vent doors on the back side of the vertical panel holder and on the lower side of the horizontal panel holder prevented pressure buildup during the tunnel start. These doors were operated electrically during tests to control the pressure differential across the panel skin.

The X-15 vertical stabilizer panels were unprotected from transient loading conditions or heating during the tunnel start or shutdown. However, no damage to the panels was discernible after completion of the tests. Each bay was vented through doors cut in the base bulkhead. In order to limit the base pressure, a large steel box was mounted close to the stabilizer base as can be seen in figure 4. The side and top surfaces of the box were parallel and in line with the side panels and closure rib of the stabilizer. The box prevented the standing tunnel shock wave (which is located just downstream of the test section at the minimum tunnel operating pressure) from affecting the stabilizer base pressure by pressure propagation upstream in the subsonic wake. As a result, the stabilizer internal bay pressure was close to the free-stream static pressure for all test conditions.

All tests were conducted at a Mach number of 3.0 and at dynamic pressures between 1,500 psf and 5,000 psf. The stagnation temperature was held constant for each run at a predetermined value between 215° F and 660° F. The dynamic pressure was varied during some tests, usually after flutter had started.

INSTRUMENTATION

Inductance-type deflectometers attached to the panel supporting structures were used to determine panel-skin deflections by measuring the change in inductance as a function of the distance between the panel skin and pickup. The pickups were positioned approximately one-quarter inch from the panel skin at locations shown in figure 7 for the two- and four-bay panels and in figure 3(a) for the vertical stabilizer. In addition, strain gages were mounted on the inside skin surface of the X-15 stabilizer in order to provide additional frequency information. Iron-constantan thermocouples were spot-welded to the panel skins at locations also shown in figures 7 and 3(a). However, for the aluminum-alloy panels, all or most of the thermocouples became detached during testing. Strain-gage-type pressure transducers were used to measure the pressures in the cavity back of the two- and four-bay panels and within the X-15 vertical stabilizer. Temperature and pressure data were recorded by means of a high-speed digital magnetic-tape recording system. Deflection data were recorded on high-speed oscillographs. In addition, motion-picture coverage of all tests was provided by high-speed 16-millimeter cameras capable of taking 3,000 frames per second. Panel skins were painted with grid lines for photographic purposes.

RESULTS AND DISCUSSION

References 2, 3, and 4 have shown that aerodynamic heating could initiate flutter of an initially flat panel under conditions of dynamic pressure and Mach number for which the unheated panel would otherwise be stable; in addition, it was found that heating could stop flutter. The basic data for this investigation are presented in table I for the two- and four-bay aluminum-alloy panels, the steel panels, and the X-15 stabilizer panels, respectively. The data tabulated for the start and termination of flutter are the dynamic pressure q, the panel differ- L
ential pressure Δp, the incremental skin temperature ΔT (a measure 1
of the midplane thermal stress for any given panel), and the modified- 6
3
thickness-ratio flutter parameter $\left(\frac{\beta E}{q}\right)^{1/3} \frac{\tau}{l}$ given by theory. Those 0
instances for which no flutter data are shown indicate either that flutter started before uniform flow conditions were established or that flutter was stopped only by termination of the test. Footnote reference marks on values of the dynamic pressure indicate increasing or decreasing dynamic pressure at the time flutter started or was terminated. The absence of a footnote reference mark indicates that q was constant and, hence, at the time flutter started or stopped, only the skin temperature was changing.

Presented in figures 8 to 11 are variations with time of model and wind-tunnel pressures and temperatures for four typical tests. The variables are shown for two tests of a two-bay aluminum-alloy panel in the horizontal panel holder, first without film cooling (fig. 8), then with film cooling (fig. 9). Figure 10 shows a typical variation of the test variables for a test of a four-bay steel panel made in the vertical panel holder after the installation of protective doors. A similar plot is shown in figure 11 for test 1 of the X-15 lower vertical stabilizer. Certain detailed results of the tests need to be examined before the overall panel flutter boundaries are discussed.

Panel Temperatures

The measured temperature data of the present investigation are incomplete because of the high thermocouple mortality rate mentioned previously. The temperatures presented in the table and figures of this report are, in many cases, based on the reading of only one thermocouple located midway between ribs. More complete temperature data presented for similar panels in reference 4, however, have shown no appreciable variation of the bay center-line temperature in the streamwise direction.

Prior to the start of a test, the panel skin and supporting structure were at essentially the same temperature. For panels that were unprotected in any way during tunnel start, the skin temperature began to rise as soon as the air started to flow (figs. 8 and 11) and increased as much as 50° F in the time required to attain test conditions. Figure 9 shows that when film cooling was used (all tests of two-bay panels except tests 2, 3, and 11), no appreciable temperature rise occurred until the water was shut off $\left(t \approx 2\frac{1}{2} \text{ seconds}\right)$. Although the protective doors (used for all tests of four-bay panels) did not provide an airtight seal from the airstream, any skin temperature increase prior to opening of the protective doors was usually insignificant.

L
1
6
3
0

The initial rapid increase in temperature of the panel skin shown in figures 8 to 11 was, of course, not typical for the supporting structure as indicated in figure 10, which shows that the temperature of the longitudinal supports increased rather slowly after the panel was exposed to the flow. Reference 4 indicated that an appreciable spanwise gradient in the skin temperature exists due to the heat-sink capacity of the longitudinal supports. Hence, the thermally induced midplane stress was not entirely uniform throughout the panel skin. This factor affects the accuracy of the calculations of panel-buckling temperature discussed in the next section.

Flutter Parameters

The panel flutter boundaries obtained in this investigation are presented in terms of the modified-thickness-ratio flutter parameter $\left(\frac{\beta E}{q}\right)^{1/3}\frac{\tau}{l}$ and the ratio of the panel-skin-temperature increment to the calculated buckling temperature $\Delta T/\Delta T_{cr}$ in the absence of airflow. The nondimensionalized temperature parameter $\frac{\alpha\,\Delta T w^2}{\tau^2}$ used in reference 4 was found to be inadequate because of differences in panel-support construction for the various panels of the investigation. For example, variations in depth of the rib channels for two- and four-bay panels appreciably affected the rotational restraint of the streamwise edges as did changes in the ratio of the panel-skin thickness to rib thickness. Variations in panel-edge rotational restraint, however, are accounted for in calculation of the buckling temperature.

The buckling temperatures presented in table I were computed with the use of the charts of reference 5 on the basis of no flow past the panel. For these calculations, the panels were treated as having an infinite length (an assumption frequently made for panels having a length greater than four times the width), and it was assumed that both the strain in the longitudinal direction ϵ_x and the stress in the lateral direction σ_y were zero. Moreover, the panel skin was assumed to be heated to a constant temperature throughout, but the panel supports were assumed to have remained at the initial prerun temperature. These last assumptions were not precisely met, as was discussed in the section entitled "Panel Temperatures"; in addition, variations in panel construction caused some uncertainty in the accuracy of the calculated buckling temperatures. For example, the spacer between the outside rib channels and the attaching heavy angle support was omitted on the four-bay aluminum-alloy panels (see fig. 1(b)); therefore, thermally induced lateral stresses may be greater for the four-bay panels than for the two-bay panels. Also, the leading and trailing edges were not fully clamped or completely fixed against thermal expansion, while the riveted attachment of the skin to supporting channels departs from the idealized attachment assumed in reference 5. Although the effects of departures from the assumptions used in calculating the buckling temperatures are not precisely known, the errors in the calculated temperatures are consistent, except possibly for those panels for which the spacers were omitted. Hence the temperature ratio $\Delta T/\Delta T_{cr}$ is considered to be a valid parameter and prior to buckling is directly proportional to the ratio of the panel midplane stress to the critical buckling stress in the absence of airflow.

L 1 6 3 0

Flutter Behavior

Observation of high-speed motion-picture film indicated that flutter for all panels was of the sinusoidal traveling-wave type, and the flutter mode appeared to be similar to the buckling mode. The aluminum-panel flutter mode consisted of approximately eight longitudinal waves and one lateral half-wave. Although the flutter and buckling modes for the steel panels appeared to be similar to those of the aluminum panels, the wave amplitudes were too small to permit certain definition. In the case of the X-15 stabilizer panels, motion-picture film coverage was inadequate for comparison of the flutter and buckling modes with those of the models. The flutter amplitudes for all panels were greatest near the trailing edges where motion, in general, was more erratic.

Throughout the investigations the deflectometer records showed the same types of flutter behavior described for the aluminum panels of reference 4. At the start of flutter of the initially flat, unbuckled panels, the motion was sinusoidal and tended to increase uniformly to a constant amplitude. After a few seconds the motion became nonuniform, beats developed, or the motion became erratic. Sometimes intermittent oscillations were noted before flutter stopped with the panel in a buckled condition. The aluminum panels (of present report) showed a tendency to develop beats (fig. 12) soon after flutter started and also to stop fluttering more abruptly. The steel panels (fig. 13) as well as the X-15 stabilizer panels, however, showed generally more erratic behavior with a reduction in frequency and intermittent oscillations near termination of flutter by buckling.

Flutter of Aluminum-Alloy Panels

L 1 6 3 0

The differential pressure was not considered to be a variable in the present investigation; however, Δp was not well controlled in all tests, as can be seen from table I. In some instances, this resulted from occurrence of flutter early in the test before adjustment of the pressures could be made. In others, inaccuracies in the indicators used to determine the adjustment necessary caused incorrect settings to be made. An attempt was made to remove at least the first-order effects of differential pressure. Because the panel loading due to differential pressure directly affects the panel midplane stress, any correction for effects of Δp should be applied directly to the temperature ratio $\Delta T/\Delta T_{cr}$, which is proportional to the stress ratio. For flat panels in compression, a differential pressure loading will reduce the midplane stress. For buckled panels the effect is less certain; however, reference 6 has shown that for a buckled panel a pressure differential can inhibit flutter.

Values of the modified-thickness-ratio flutter parameter $\left(\frac{\beta E}{q}\right)^{1/3} \frac{\tau}{l}$ were plotted against the values of the temperature ratio $\Delta T/\Delta T_{cr}$; the values of $\Delta T/\Delta T_{cr}$ were obtained from table I and are uncorrected for Δp. Curves were faired through the plotted data and emphasis was placed on data points at or near zero Δp. The differences between the flutter-start data points and the faired curve are plotted in figure 14(a) as a function of the absolute value of Δp. This figure shows a definite trend in the variation of the incremental value of the temperature ratio with $|\Delta p|$. The curve drawn through the data points of figure 14(a) was used to determine correction factors which were applied to the original values of $\Delta T/\Delta T_{cr}$ obtained from table I. The modified thickness ratio is plotted against corrected values of $\Delta T/\Delta T_{cr}$ in figure 14(b).

Effects of aerodynamic heating.- Figure 14(b) shows the effects of aerodynamic heating on the flutter of aluminum-alloy, multibay panels. The open symbols show the start of flutter resulting from increases in panel temperature or in dynamic pressure, or in both. The solid symbols show the conditions at which flutter was terminated by further increases in panel temperature or decreases in dynamic pressure. Two distinctly different flutter boundaries, similar to those found in reference 4, are described by the open and solid symbols. As was the case in this reference, the open symbols define the flat-panel flutter boundary, since no buckling prior to the start of flutter was evidenced in the deflectometer records or high-speed motion pictures. The boundary described by the solid symbols separates a region of flutter from a region in which the panels were buckled and stable. As shown in reference 4, this latter boundary may be approached from above and is therefore the buckled-panel flutter boundary. Since the temperature ratio used in figure 14 is proportional to the ratio of the panel mid-plane stress to the stress required to buckle the panel in the absence of airflow, the flutter boundaries may be interpreted in terms of the panel stress. The figure shows that the flat-panel boundary is characterized by an increase in thickness required to prevent flutter with an increase in thermally induced stress, whereas the buckled-panel boundary shows a decrease in required thickness with increasing thermal stress.

L
1
6
3
0

Outside of the flutter region, conditions for actual buckling of the panel are undefined except in the immediate vicinity of the intersection of the flat-panel and buckled-panel boundaries. It may be noted that this intersection or transition peak occurs at temperatures greater than the calculated buckling temperature in the absence of airflow and, hence, supports the premise of reference 7 that the presence of supersonic flow tends to suppress panel buckling. The transition peak occurs at values of the flutter parameter 60 percent in excess of the extrapolated value for an unheated panel and thus represents a large increase of thickness required to prevent flutter in the presence of aerodynamic heating.

The data for two-bay and four-bay panels in figure 14(b) show no systematic differences within the scatter of the data and apparently have the same flutter boundaries. No differences would be expected as long as individual bays can be considered as individual panels and adequate compensation for differences in construction is provided by the parameters. Actually, the differences in fabrication, together with inaccuracies in temperature measurements and in compensation for differences in the pressure differential across the panel, are believed to contribute most to the scatter.

Effects of panel stiffeners.- A few tests of the effectiveness of simple stiffeners for prevention of flutter were made. Each bay of a 2-A panel was modified with a Z-section stiffener placed crosswise to the flow direction at the midlength location. One flange of the Z-section was attached to the skin by a single row of rivets and the other flange was riveted to one of the steel crossmembers of the frame; however, the webs of the Z-sections were not attached directly to the longitudinal channels. Such conditions probably imposed little rotational restraint on the panel skin at the line of attachment. The results are shown in figure 15, which also reproduces the faired boundaries from figure 14(b). No appreciable effect on the flutter boundaries was shown by the "start" or "end of flutter" symbols, and the lateral stiffener was, therefore, completely ineffective in stiffening the panel against flutter.

A single angle stiffener was riveted to the panel skin along the longitudinal center line of each bay. The stiffener was 7/16 inch deep and was supported only by the skin. Although the stiffener weight was only 28 percent that of the panel skin, the moment of inertia of the skin plus stiffener was 135 times that of the skin alone (based on the original panel width). The data show that stiffening the panel greatly increased its resistance to flutter in the original mode. Flutter was successfully prevented for the test conditions as shown by the dashed line in figure 15. Values of the parameters are based on the dimensions and calculated buckling temperature of the original, unstiffened panel and, therefore, represent the higher dynamic pressure for which flutter was prevented. This increase in dynamic pressure for which flutter was prevented was substantially greater than would be indicated by the flutter correlation of reference 2 if the stiffener was assumed to reduce effectively the individual panel width by a factor of one-half. Hence, if it is assumed that further heating of the panel would not cause flutter, some deficiency of the flutter correlation of reference 2 is indicated.

L
1
6
3
0

Edge restraint.- Unexpectedly large differences in flutter characteristics, resulting from apparently minor differences in panel-support construction, are shown in figure 16, which compares the flutter boundaries of figure 14(b) with those reported in reference 4. The investigation of reference 4 was carried out concurrently with the present investigation and the panels tested were similar to the four-bay aluminum panels of the present tests, except for the support of the leading and trailing edges. For the panels of reference 4, the leading- and trailing-edge Z-sections were supported from the mounting fixture by means of a steel angle bolted to the Z-section web. This arrangement imposed less restraint on thermal elongation, at least locally, than was the case for the panels of the present investigation. However, the skins were riveted to the longitudinal channels for both series of panels so that restraint on thermal elongation of the panel skin by the relatively cool supports was the same over most of the panel length. In calculation of the critical buckling temperatures used in figure 16, the same assumptions were made for both series of panels; that is, lateral expansion was unrestrained, whereas longitudinal expansion was prohibited ($\sigma_y = 0$, $\epsilon_x = 0$). Consequently, the differences in panel construction are reflected in the data.

Figure 16 shows that the flat-panel flutter boundaries for both series of panels were in close agreement up to the transition point of the data for the present tests. However, the post-buckling boundaries differed greatly with the result that peak values of the modified-thickness-ratio flutter parameter were about one-third greater for the panels of reference 4 and occurred at higher values of the temperature ratio. These results cannot be adequately explained at present; however, the differences in panel restraints indicate some factors which may be responsible.

The edge rotational restraints were much the same for both series of panels because of the similar type of construction. However, the restraint against lateral expansion was such that appreciable lateral stress could develop in the panels of reference 4. This lateral restraint, coupled with the partial restraint against longitudinal expansion, could well have resulted in significantly larger values of the stress ratio σ_y/σ_x prior to buckling or flutter than would be expected for the panels of the present report. Changes in panel restraints affecting the stress ratio are known to have large effects on panel-buckling coefficients and can change even the buckling mode. Hence, appreciable effects of stress ratio on the flutter speed could be expected, particularly at transition from the flat-panel to buckled-panel flutter boundaries and in the post-buckled range. Unfortunately, present flutter theories are inadequate in describing the experimentally observed flutter modes and hence yield little definite information on how flutter characteristics should be affected. It should be pointed out that although the experimental flutter modes of the panels of the present investigation and those of reference 4 appeared to be similar, discrimination of the exact number of half-waves between about 13 and 16 could not be accomplished because of the high frequency of the motion (table I) and the quality of the available instrumentation.

L
1
6
3
0

Figure 16 shows that actual buckling in the stable region immediately adjacent to the peak of the curves occurred at appreciably higher temperatures for the panels of reference 4 than for the panels of the present report. This difference could be accounted for if the leading- and trailing-edge supports for the panels of reference 4 permitted sufficient relief of the streamwise thermal stress. However, calculations of critical buckling temperatures based on expansion at the leading and trailing edges for the panels of reference 4 account for only about 20 percent of the difference in the temperature-ratio parameter shown in figure 16. On the other hand, the greater spanwise restraint $\left(\sigma_y \neq 0\right)$ for the panels of reference 4 would reduce the reference buckling temperatures and increase the separation of the two peaks of figure 16.

Flutter of Steel Panels

Table I shows that the differential pressure for the start of flutter of the 17-7 PH stainless-steel panels was generally large and, consequently, the procedure used for correcting the temperature-ratio parameter of the aluminum panels could not be applied to these data. Corrections determined from figure 14(b) were arbitrarily applied to these data and are, at least, justified by some reduction in scatter in the resulting plot shown in figure 17. The panel-skin supports were made of aluminum alloy and in some cases were the identical supports used for the aluminum-skin panels discussed previously. (See fig. 1(b).) The steel-panel boundaries, however, show a much smaller change in the flutter parameter $\left(\frac{\beta E}{q}\right)^{1/3} \frac{\tau}{l}$ with temperature ratio than did the aluminum-alloy panels. This was true for both the flat- and buckled-panel boundaries. The flat-panel boundary shows that for constant aerodynamic conditions only a 10-percent increase in panel thickness is required to prevent flutter due to aerodynamic heating as compared with 60 percent for the aluminum-alloy panels. (See fig. 14.) The transition peak between the flat- and buckled-panel boundaries, however, occurred at about the same value of temperature ratio for the steel- and aluminum-alloy panels. Flutter modes appeared similar, but could not be definitely established to have the same number of half-waves, because the amplitudes were much smaller for the steel panels than for the aluminum panels.

L
1
6
3
0

Reasons for differences in slope of the flutter boundaries are not presently known. It should be pointed out, however, that although the lateral stress σ_y is believed to have been small and to have had negligible effect on the calculated values of ΔT_{cr}, the edge rotational restraint and the stress ratio σ_y/σ_x were necessarily different for aluminum and steel skins when applied to the same panel supports. Conceivably, the stress ratio could directly affect the flutter dynamic pressure with negligible change in temperature ratio. The panel skins were made of the minimum-gage material available, and flutter occurred near the maximum dynamic pressure of the tunnel so that values of the parameter smaller than those shown in figure 17 were, therefore, unattainable. However, the area above the flutter boundaries of figure 17 was thoroughly explored by tests not listed in this report, and there was no evidence of flutter.

Flutter of X-15 Stabilizer Panels

Effect of aerodynamic heating.- Results of tests of the X-15 vertical-stabilizer panels with length-width ratio of 10 are shown in figure 18. These data are presented in terms of the temperature increment ΔT rather than the temperature ratio, because reliable calculated buckling temperatures were not available. The edge rotational restraint of the X-15 tail panels was believed to be not greatly different from that of the 17-7 PH stainless-steel panels. That is, the edge rotational restraints approached more nearly a clamped condition than a simply supported condition. The corrugated ribs to which the skin was attached L
provided considerably less restraint to thermal elongation than did the 1
longitudinal channels of the 17-7 PH stainless-steel panels. Consequently, 6
direct comparison of the results is questionable. The data are pre- 3
sented, however, because they do represent full-scale results and the 0
material properties of Inconel X are not greatly different from those of 17-7 PH stainless steel over the temperature range of the investigation. The data of figure 18 show about the same increase in the modified-thickness-ratio parameter from the cold or unstressed condition (obtained by extrapolation) to the transition peak between the flat- and buckled-panel boundaries. The general level of the data for the vertical tail panels is, however, slightly lower than that for the 17-7 PH stainless-steel panels.

Although the aluminum and steel panels were not intended as scaled models of X-15 panels, it is apparent that widely divergent flutter results may be obtained from tests of model panels unless model and prototype are made of the same material, have the same edge restraints, and the same ratio of lateral to longitudinal stress.

Panel stiffeners.- In order to provide the required flutter margin for the X-15 stabilizer side panels, stiffeners were riveted along the lateral and longitudinal center lines of each bay. The stiffeners were 0.030-inch-thick, 15/16-inch-deep Inconel X channels. Although the stiffener weight was only one-third that of the panel skin, the moment of inertia of the stiffener and skin was increased by a factor of 1,000. Such an increase in stiffness would imply a 10-fold increase in the modified-thickness-ratio parameter, placing it well out of the flutter region. If, however, the stiffener was assumed to subdivide effectively each panel bay into four equal individual panels, then each panel would have the same length-width ratio as the original panel, but twice the thickness-length ratio. In this case, the modified thickness ratio is only doubled but would still provide an adequate flutter margin.

A single test was made at a dynamic pressure of 3,200 psf and a stagnation temperature of 500° F without evidence of panel flutter. A trace of the variation of the thickness-ratio parameter with increase in skin temperature for this test is shown by the dashed line in figure 18.

Values of the parameter are based on the unstiffened-panel dimensions and, as is shown by the figure, are well within the region of the unstiffened-panel boundary. The channel stiffeners are now incorporated in the production models of the X-15 stabilizer.

CONCLUDING REMARKS

A flutter investigation of aerodynamically heated multibay aluminum-alloy and stainless-steel panels with length-width ratios of 10 has been made at a Mach number of 3.0. The panels were restrained against thermal expansion at the leading and trailing edges but permitted expansion and some rotation along the streamwise edges. In addition, flutter results were obtained for the full-scale X-15 vertical-stabilizer panels with length-width ratio of 10.

All panels showed flutter boundaries characterized by diverse trends for the panel conditions prior to and following thermal buckling. In the flat, unbuckled condition, the panel thickness required to prevent flutter increased with increasing thermally induced stress. Post-buckled flutter boundaries showed a decreasing thickness required to prevent flutter for further increases in thermal stress. The flutter boundaries for the cold or unstressed condition (obtained by extrapolation) showed good agreement for all panels considered. The peak thickness required to prevent flutter in the presence of aerodynamic heating occurred at the transition between the flat-panel boundary and the buckled-panel boundary. This peak value (for aluminum-alloy panels) was as much as 60 percent greater than the extrapolated value for an unheated, unloaded panel.

Peak values of the modified-thickness-ratio flutter parameter for the aluminum-alloy panels were about one-third less than for the panels of NASA Technical Note D-921 which differed principally in skin-support construction. Differences in the panel-skin supports resulted in somewhat greater ratios of lateral to longitudinal stress σ_y/σ_x for the heated panels of NASA Technical Note D-921.

The flutter boundary for the 17-7 PH stainless-steel panels was relatively unaffected by aerodynamic heating prior to thermal buckling, with the result that peak values of the flutter parameters were only about 10 percent greater than that for the cold or unstressed condition. Differences in the results of the steel panels and the aluminum-alloy panels may be attributed to differences in edge rotational restraint, stress ratio σ_y/σ_x, or, possibly, the large values of pressure differential that existed across the steel panels during tests.

Flutter results for the X-15 stabilizer panels with length-width ratio of 10 showed about the same magnitude increase in the flutter parameter due to aerodynamic heating prior to buckling as was shown for the steel panels. Direct comparison of flutter results, however, is questionable because of differences in edge rotational restraints and in the ratio of lateral to longitudinal stress in the panels.

Stiffeners were found to be effective in decreasing the susceptibility to panel flutter if they were oriented parallel to the direction of flow.

L
1

Langley Research Center, 6
National Aeronautics and Space Administration, 3
Langley Station, Hampton, Va., March 29, 1962. 0

REFERENCES

L1630

1. Kordes, Eldon E., and Noll, Richard B.: Flight Flutter Results for Flat Rectangular Panels. NASA TN D-1058, 1962.

2. Kordes, Eldon E., Tuovila, Weimer J., and Guy, Lawrence D.: Flutter Research on Skin Panels. NASA TN D-451, 1960.

3. Guy, Lawrence D.: The Effects of Aerodynamic Heating on Panel Flutter. Symposium Proceedings Structural Dynamics of High-Speed Flight, ACR-62, vol. 2, Aircraft Industries Assoc. and Office Naval Res., April 1961.

4. Dixon, Sidney C., Griffith, George E., and Bohon, Herman L.: Experimental Investigation at Mach Number 3.0 of the Effects of Thermal Stress and Buckling on the Flutter of Four-Bay Aluminum Alloy Panels With Length-Width Ratios of 10. NASA TN D-921, 1961.

5. Peterson, James P., and Whitley, Ralph O.: Local Buckling of Longitudinally Stiffened Curved Plates. NASA TN D-750, 1961.

6. Sylvester, Maurice A.: Experimental Studies of Flutter of Buckled Rectangular Panels at Mach Numbers From 1.2 to 3.0 Including Effects of Pressure Differential and of Panel Width-Length Ratio. NASA TN D-833, 1961. (Supersedes NACA RM L55I30.)

7. Hedgepeth, John M.: Flutter of Rectangular Simply Supported Panels at High Supersonic Speeds. Jour. Aero. Sci., vol. 24, no. 8, Aug. 1957, pp. 563-573, 586.

TABLE I.- PANEL FLUTTER DATA

Panel	Test	τ, in.	l, in.	ΔT_{cr}, °F	T_t, °F	f, cps	Start of flutter				End of flutter			
							q, psf	ΔT, °F	Δp, psi	$\left(\frac{\beta E}{q}\right)^{1/3}\frac{\tau}{l}$	q, psf	ΔT, °F	Δp, psi	$\left(\frac{\beta E}{q}\right)^{1/3}\frac{\tau}{l}$
Aluminum-alloy panel; E = 10.5×10^6 psi														
2-A	1	0.025	27	43.1	400	790	3,700	25	-0.2	0.097	------	---	-----	-----
	2	.032	27	70.0	410	---	3,220	105	1.6	.130	3,220	115	1.5	0.130
	3	.032	27	70.0	410	820	3,285	80	0	.129	3,160	125	0	.131
	4	.032	27	70.0	404	840	[a]3,285	82	0	.129	3,220	137	-.1	.130
	5	.032	27	70.0	400	910	[b]4,420	60	.21	.117	------	---	-----	-----
	6	.032	27	70.0	495	880	4,510	60	1.1	.116	[b]4,500	200	-.2	.116
4-A	7	0.025	26	43.5	640	695	3,100	45	1.2	0.107	3,360	230	-0.2	0.104
	8	.025	26	43.5	215	720	5,010	20	-1.7	.091	------	---	-----	-----
	9	.025	26	43.5	300	650	3,010	31	-.14	.108	------	---	-----	-----
	10	.025	26	43.5	630	630	2,000	53	-.6	.124	2,000	87	.42	.124
2-A	[c]11	0.032	27	----	415	770	3,265	90	-0.3	0.129	3,370	120	-0.6	0.128
	[d]12	.025	27	----	407	---	3,280	---	-----	-----	4,950	---	-----	-----
Steel panel; E = 29×10^6 psi														
2-S	1	0.020	27	62.5	650	520	4,900	66	0.26	0.099	4,750	143	0.20	0.100
4-S_1	2	.020	26	65	500	445	4,940	94	.49	.103	4,940	101	.49	.103
4-S_2	3	.020	28	58	400	560	4,940	23	.68	.095	4,830	133	.24	.096
4-S_2	4	.020	28	58	404	565	4,940	15	.69	.095	4,830	159	.43	.096
4-S_2	5	.020	28	58	400	440	4,150	16	.66	.101	4,150	86	.69	.101
4-S_2	6	.020	28	58	495	540	4,830	13	.15	.096	4,830	133	.46	.096
4-S_1	7	.020	26	65	400	500	------	---	-----	-----	5,020	92	-.56	.102
X-15 stabilizer panel; E = 31×10^6 psi														
----	1	0.030	66	----	450	480	[b]1,730	19	0.32	0.087	1,500	66	0.20	0.092
----	2	.030	66	----	436	250	1,560	30	.19	.090	[b]1,730	180	-.11	.087
----	3	.030	66	----	440	220	[a]1,760	10	.03	.086	[b]1,670	234	-.05	.088

[a]Dynamic pressure increasing.
[b]Dynamic pressure decreasing.
[c]Lateral web along center line of each bay.
[d]Longitudinal angle along center line of each bay.

L-1630

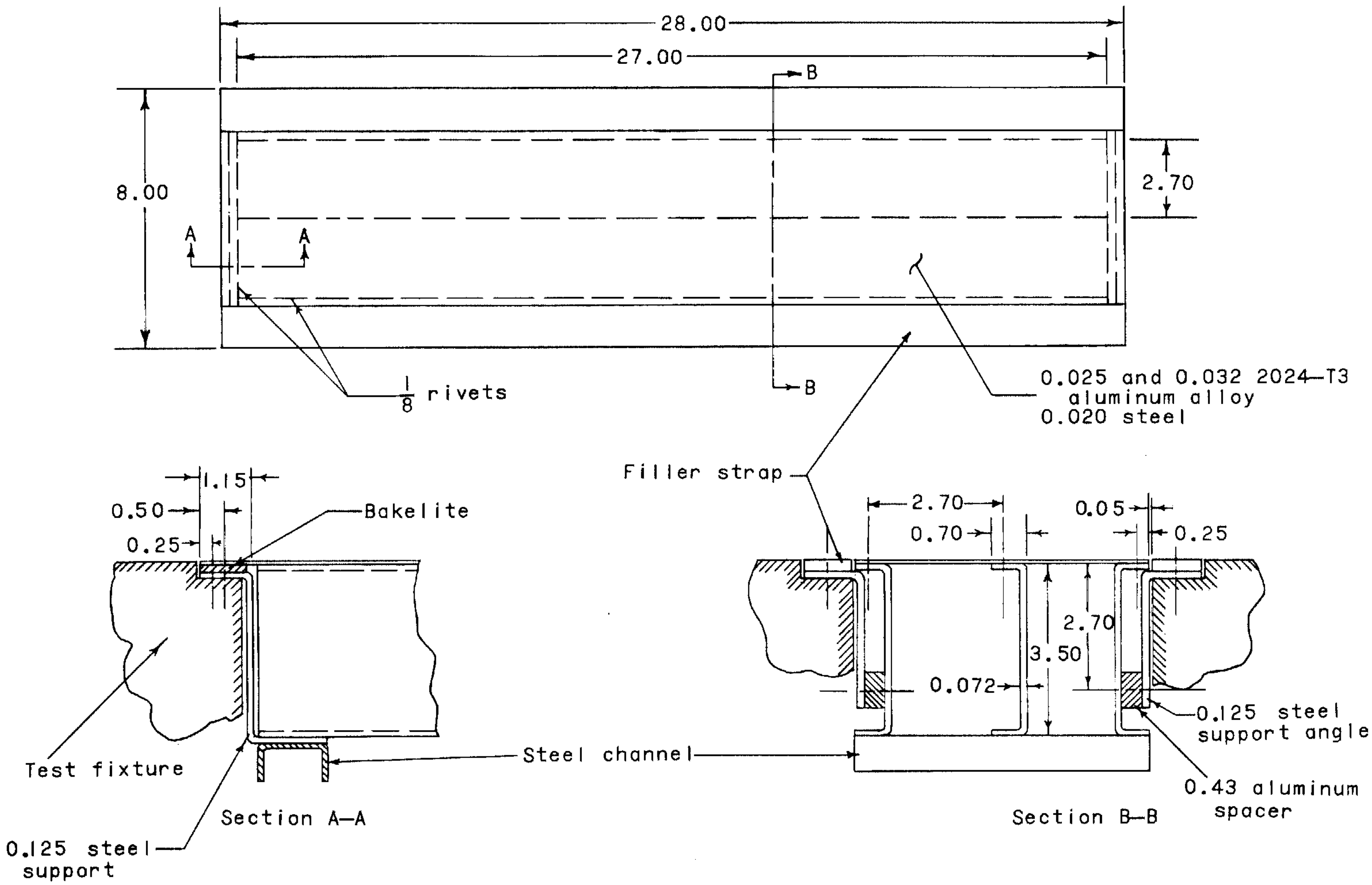

(a) Two-bay aluminum-alloy (2-A) and steel (2-S) test panels.

Figure 1.- Construction details of test panels. All dimensions are in inches.

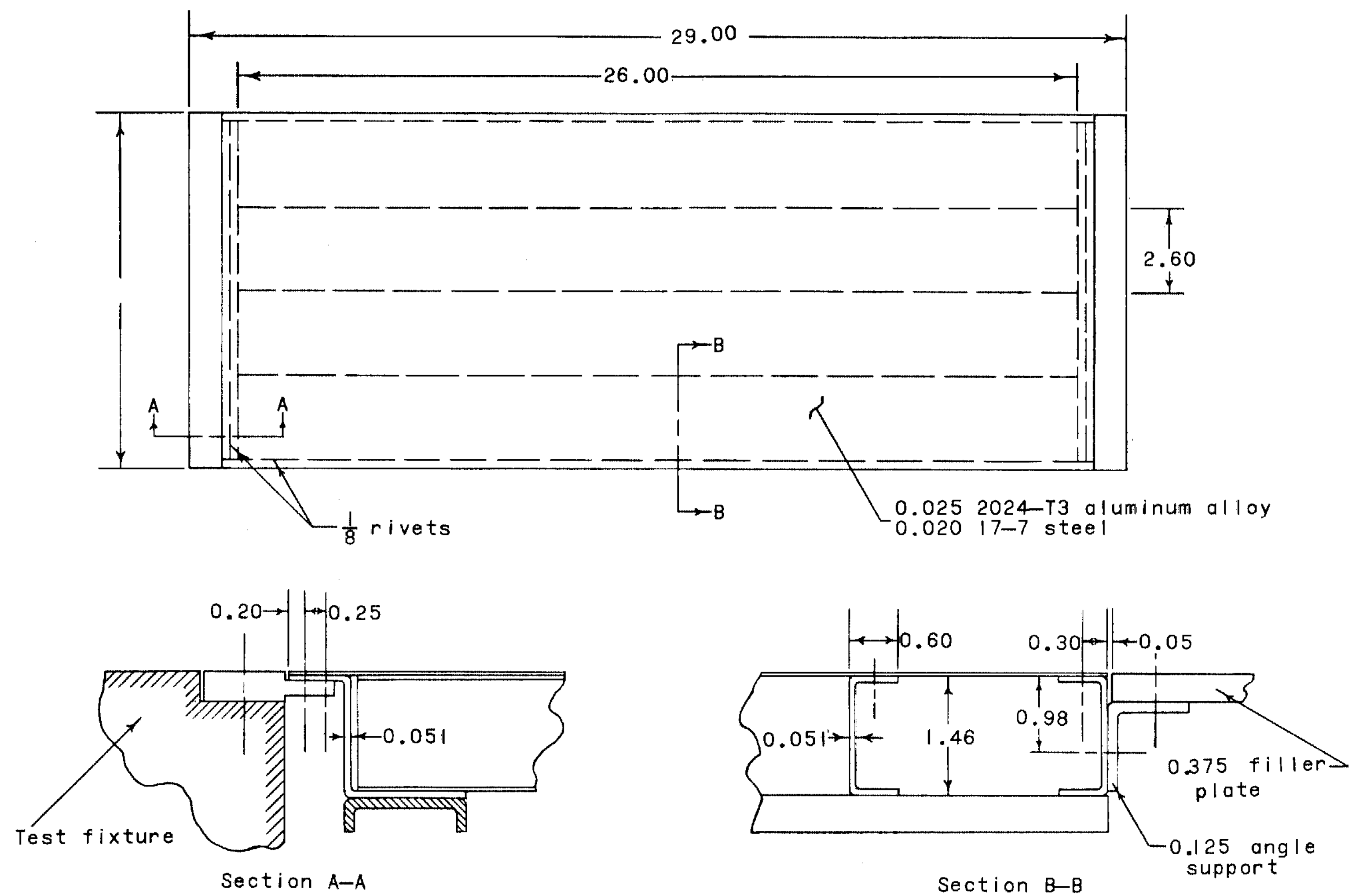

(b) Four-bay aluminum-alloy (4-A) and stainless-steel (4-S_1) test panels.

Figure 1.- Continued.

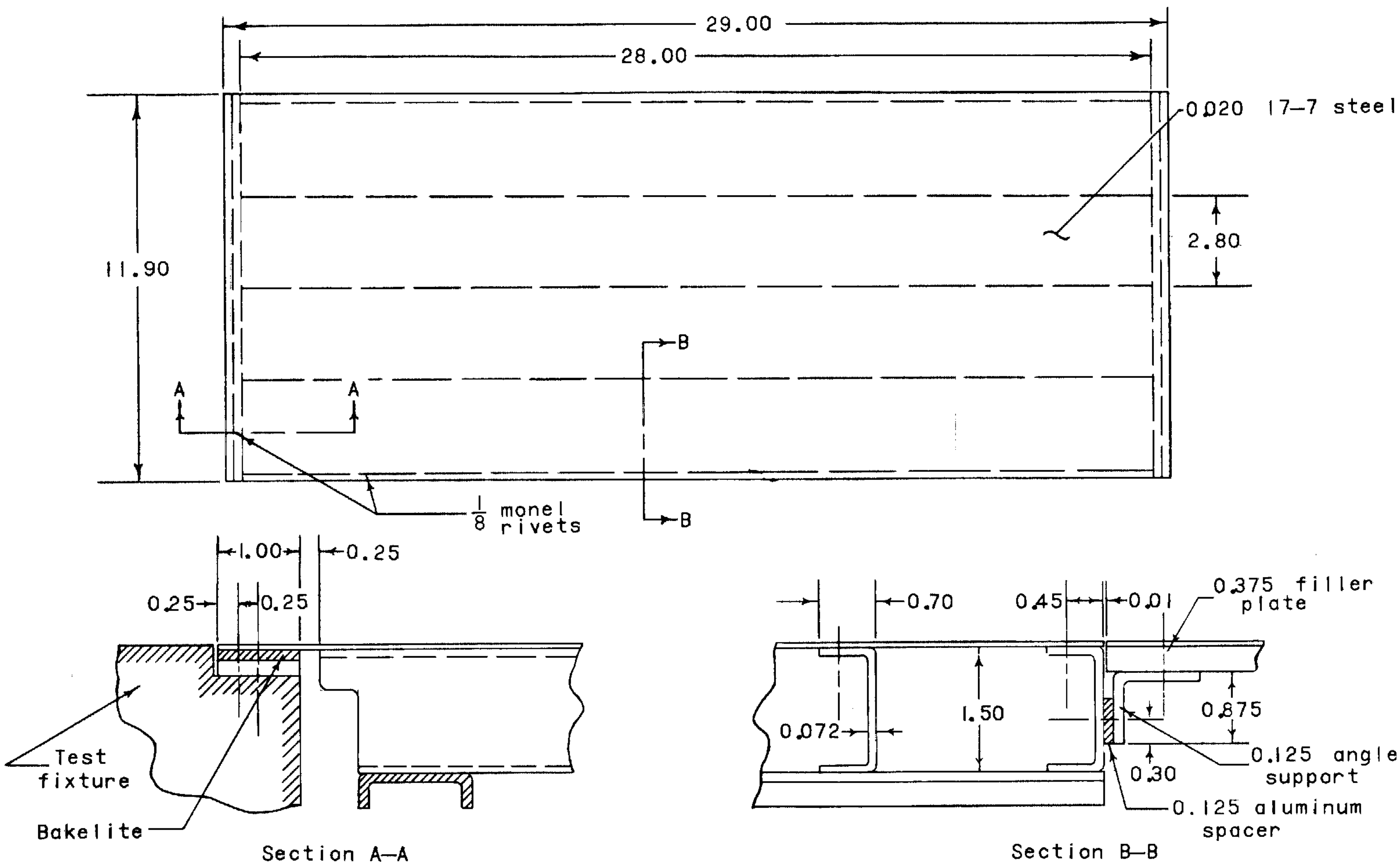

(c) Four-bay stainless-steel panel (4-S_2) with aluminum frame.

Figure 1.- Concluded.

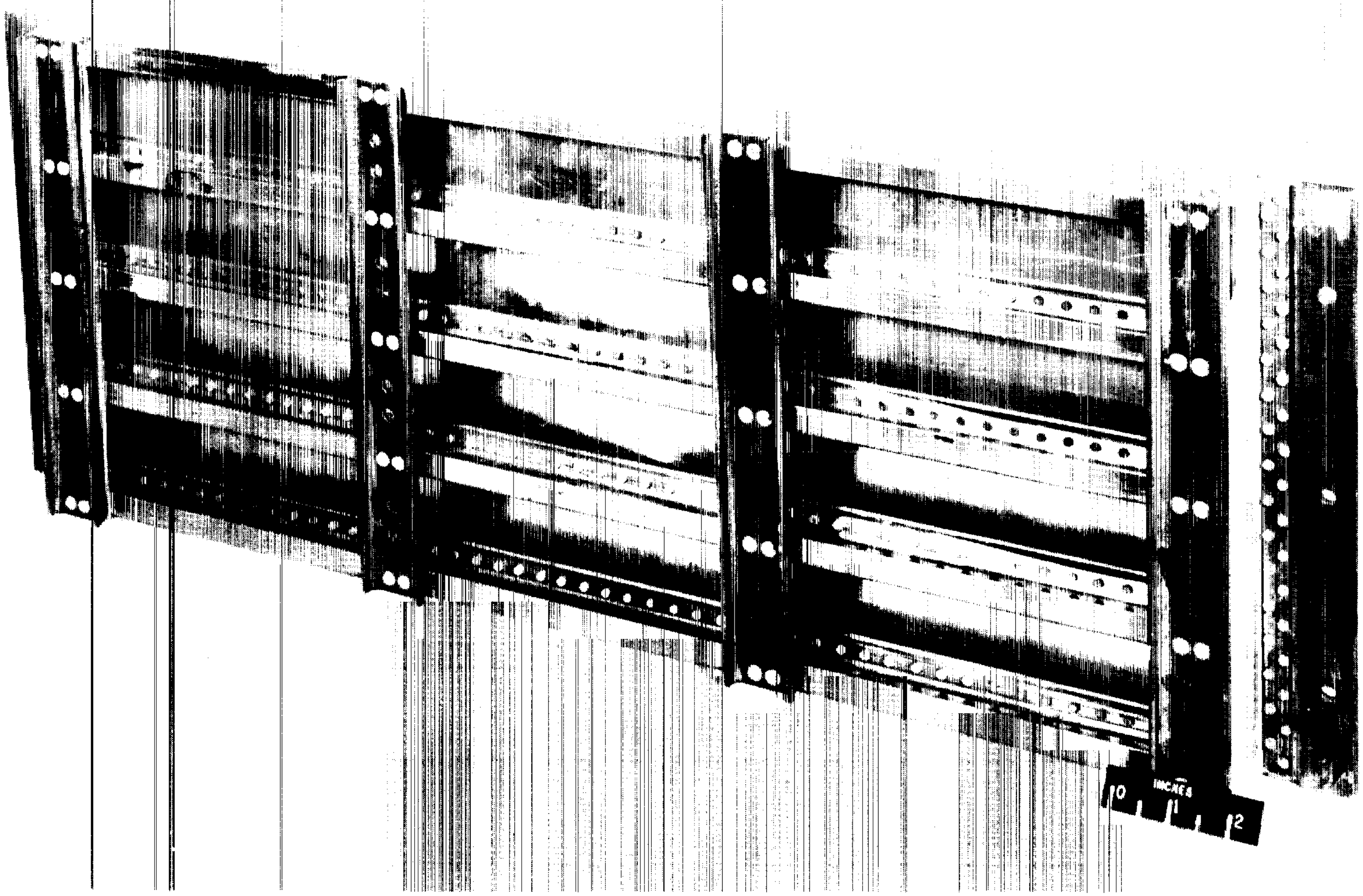

Figure 2.- Rear view of panel 4-A. L-61-3927.1

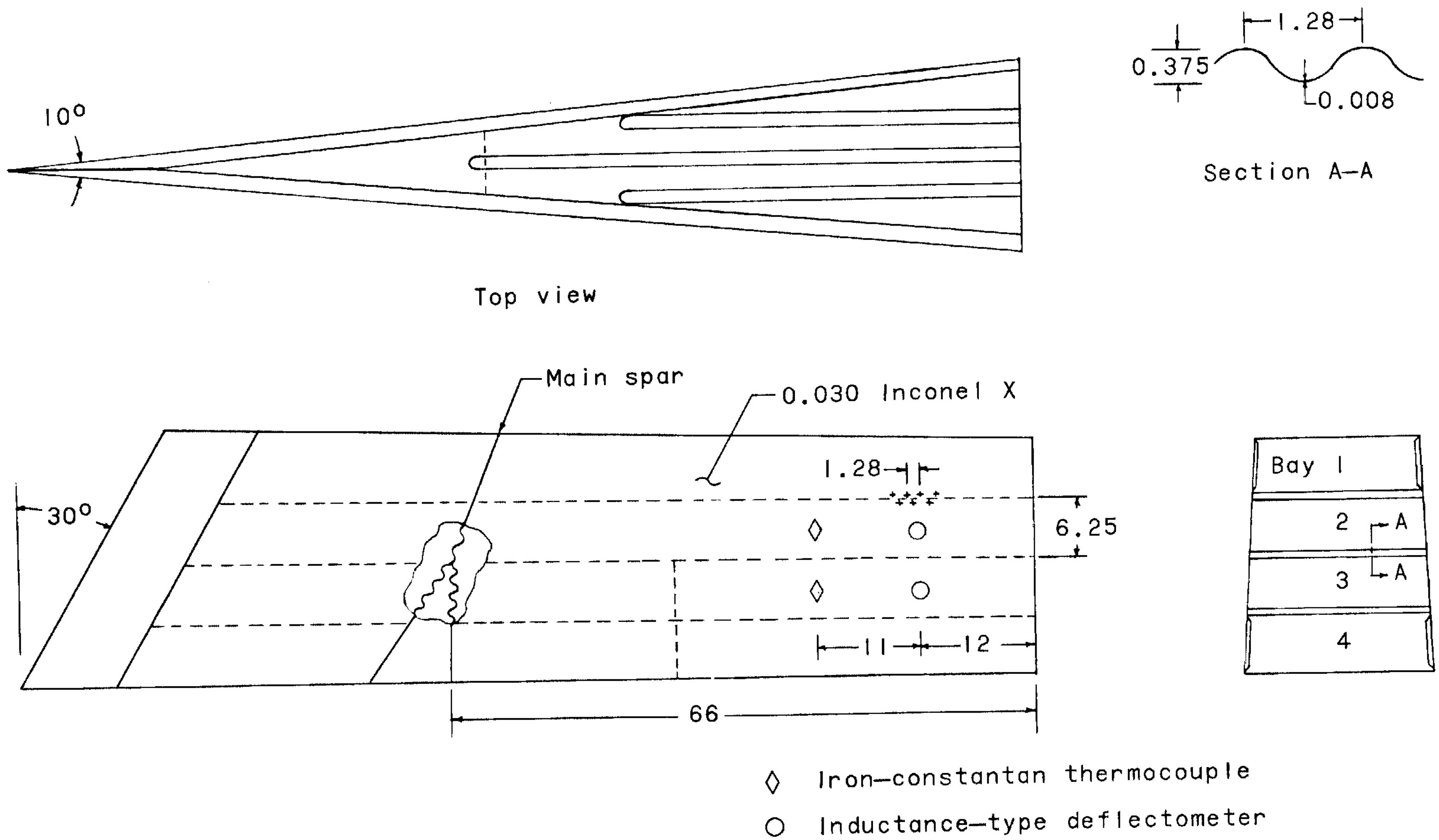

(a) Lower vertical X-15 stabilizer.

Figure 3.- Panel construction details of all-movable vertical stabilizer of X-15 airplane. All dimensions are in inches.

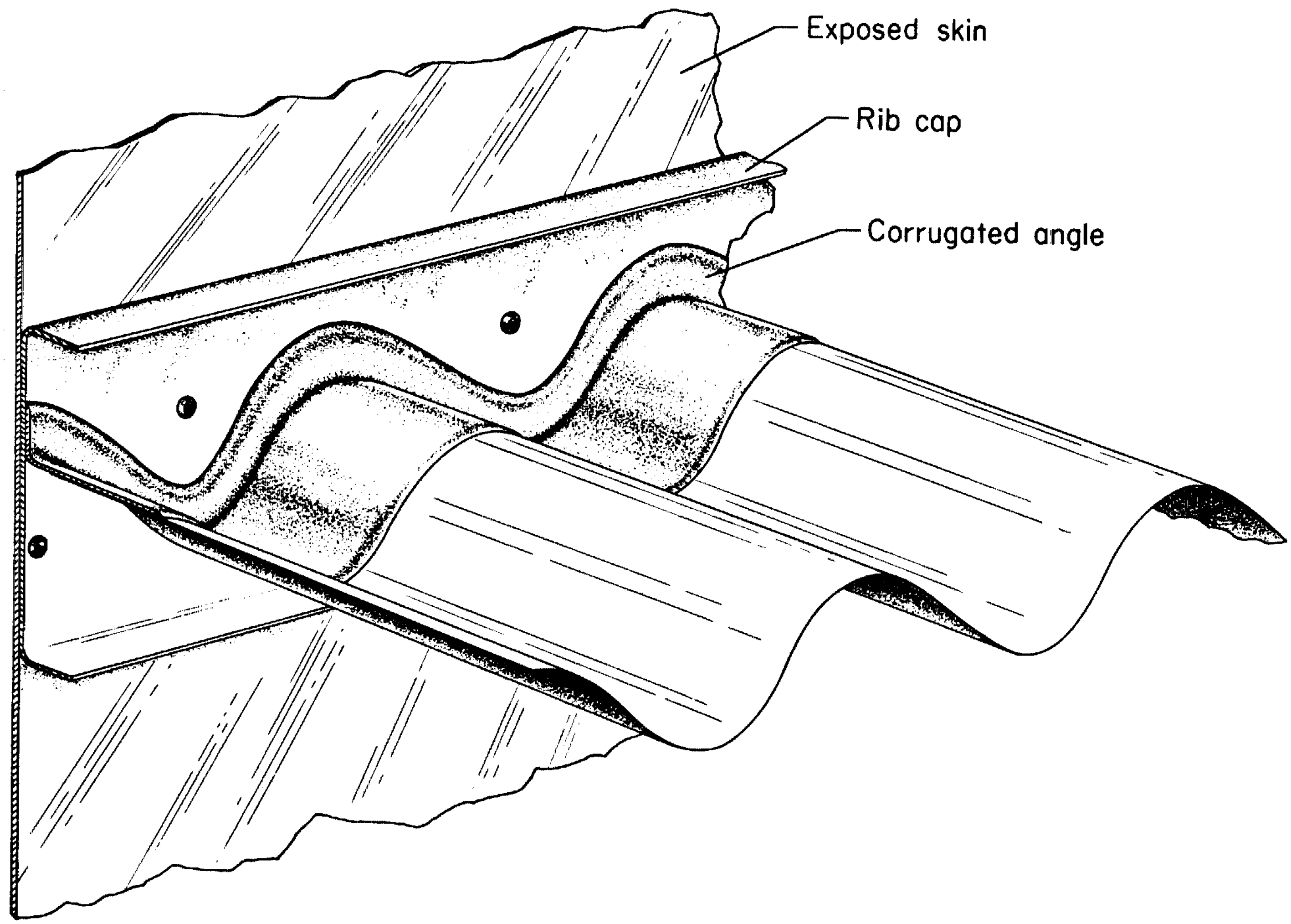

(b) View of internal rib attachment.

Figure 3.- Concluded.

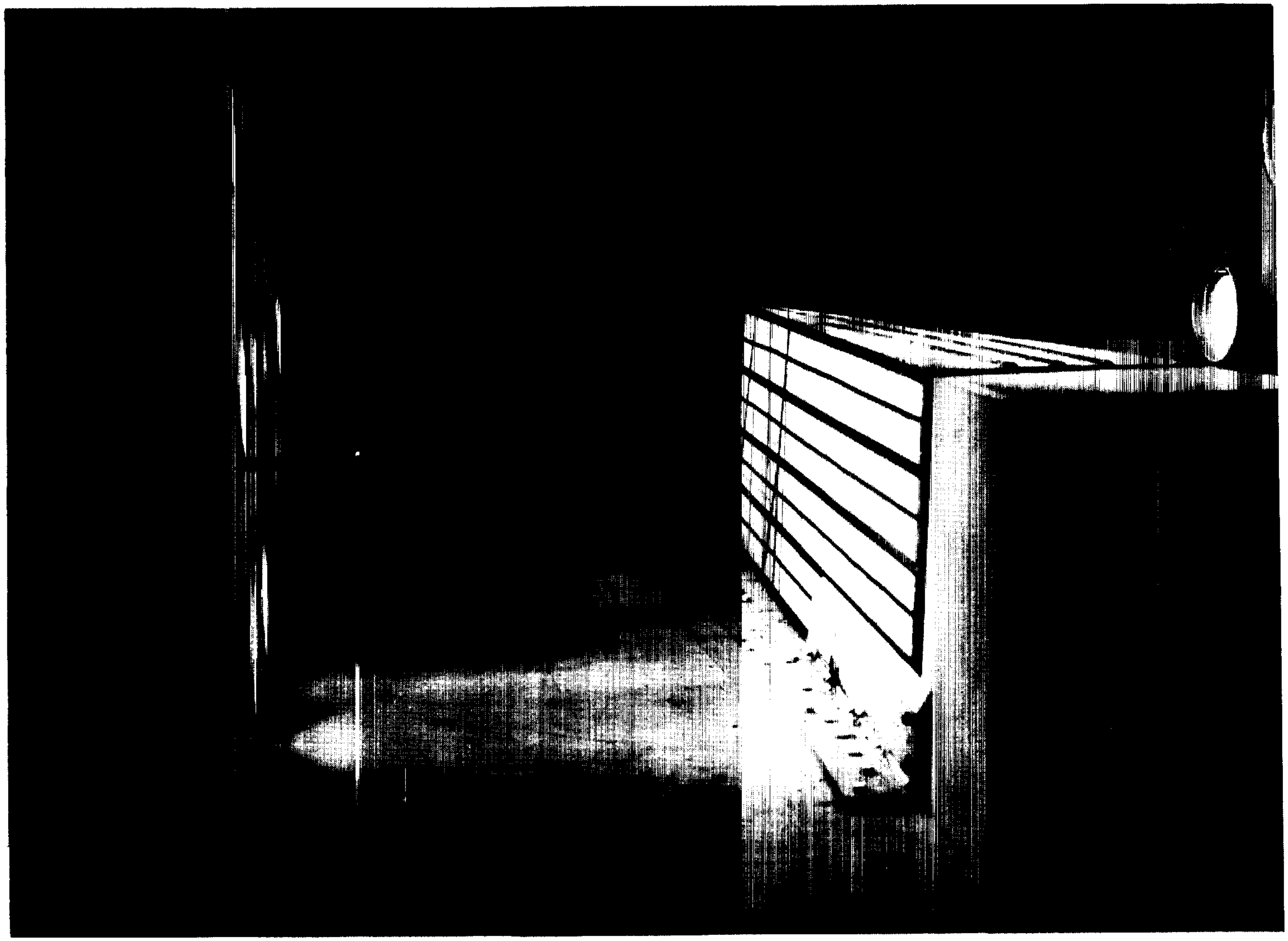

L-60-6523
Figure 4.- X-15 vertical stabilizer mounted in tunnel test section, as viewed from downstream.

L-1630

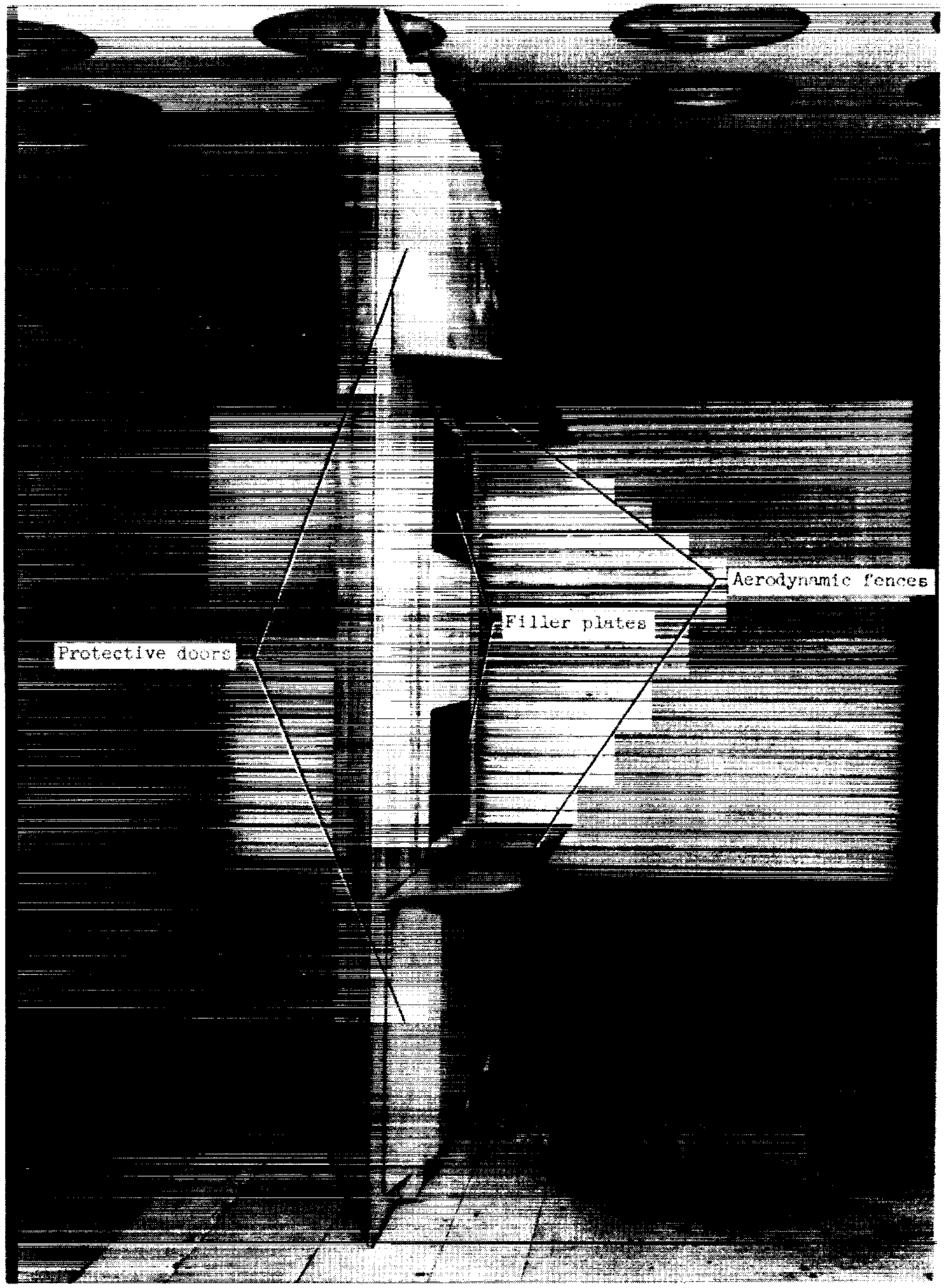

L-60-1859.1

Figure 5.- Panel mounted in vertical panel holder, as viewed from upstream. Protective doors are in open position.

L-1630

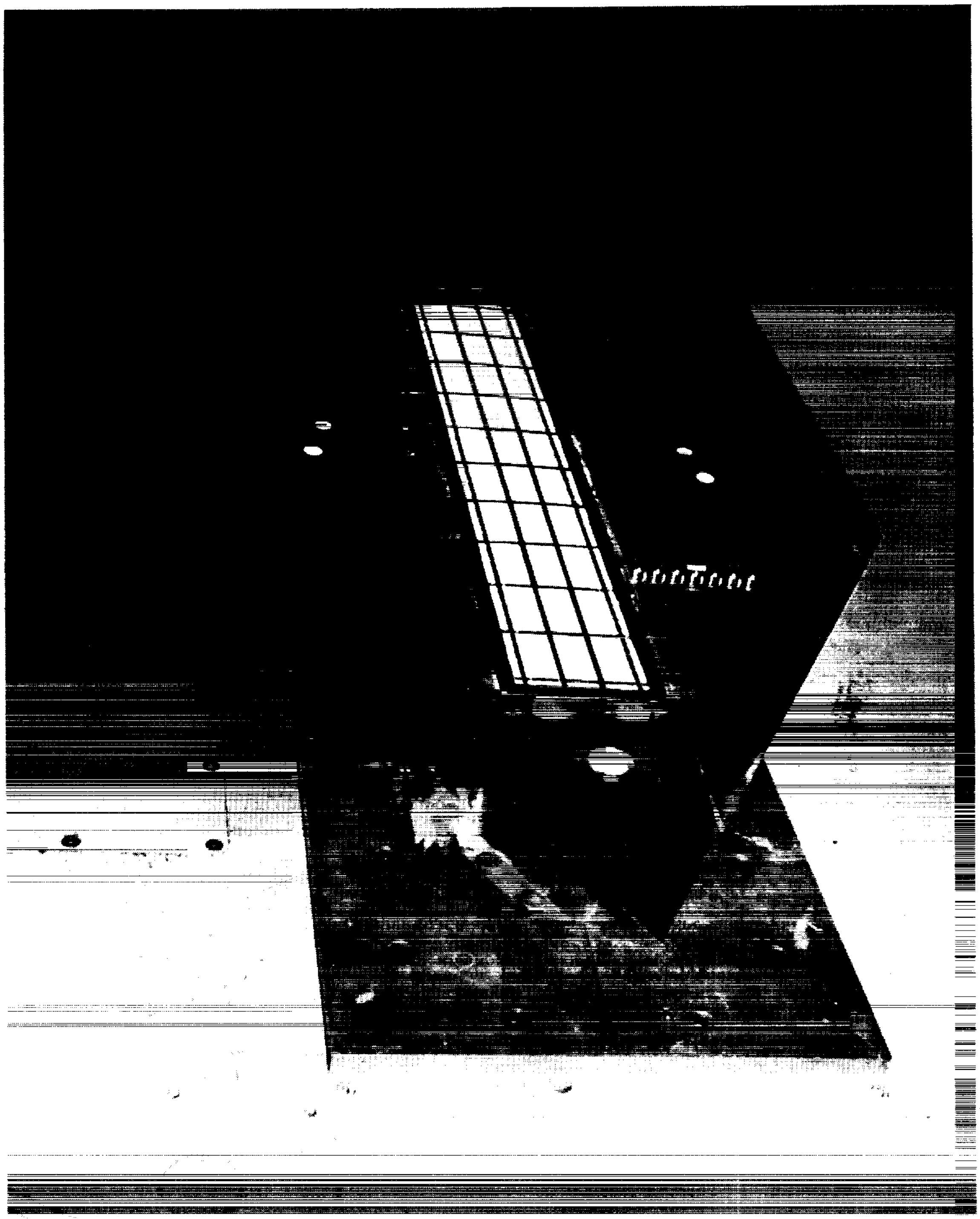

L-59-8116.1

Figure 6.- Panel mounted in horizontal panel holder, as viewed from downstream.

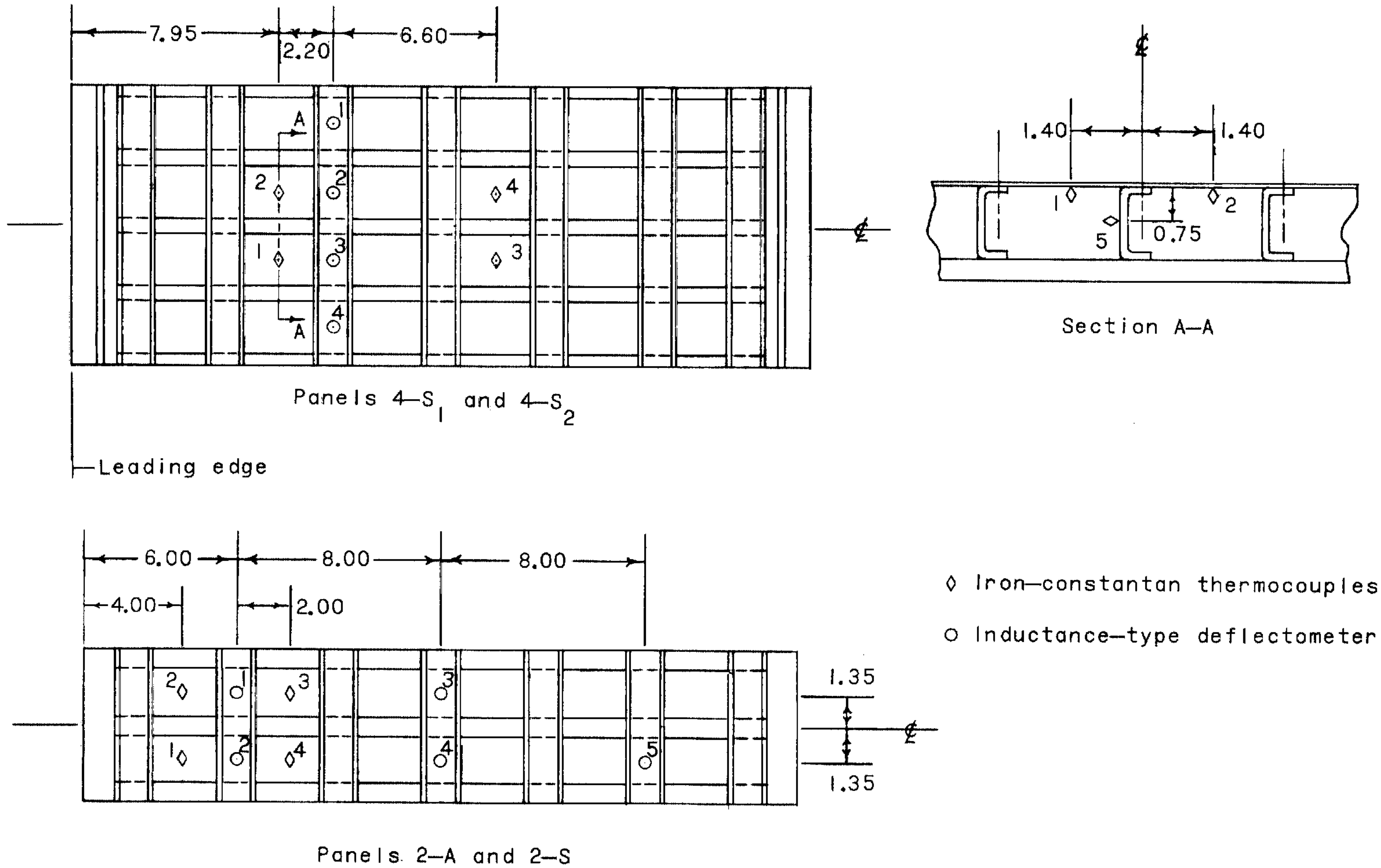

Figure 7.- Location of panel instrumentation. All dimensions are in inches.

L-1630

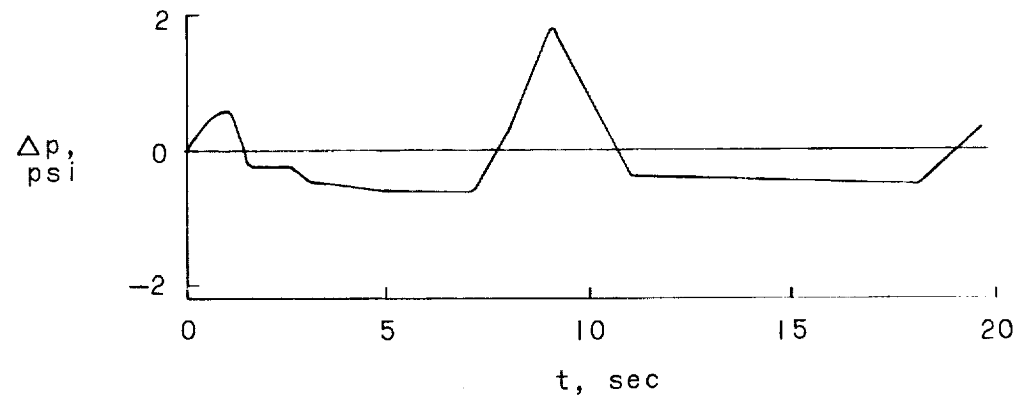

(a) Variation of differential pressure with time.

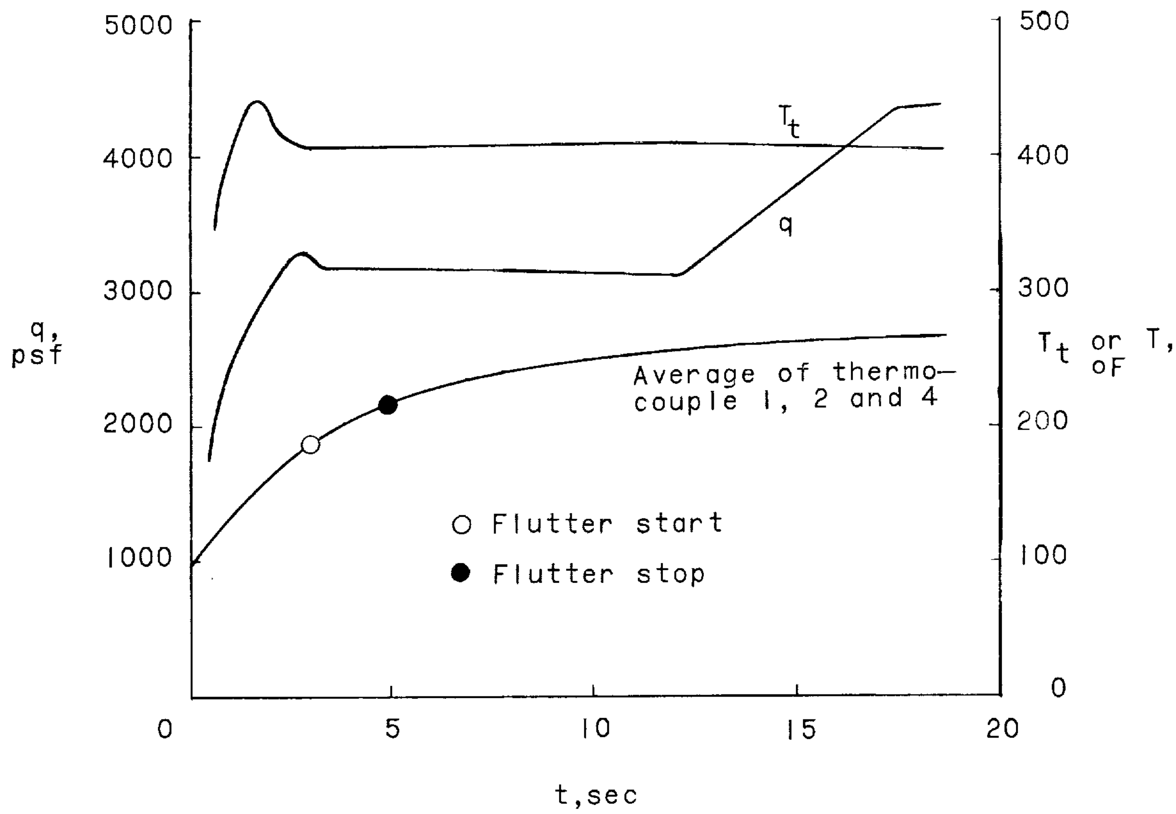

(b) Variation of dynamic pressure, stagnation temperature, and skin temperature with time.

Figure 8.- Test conditions of two-bay aluminum-alloy panel. (Test 11.)

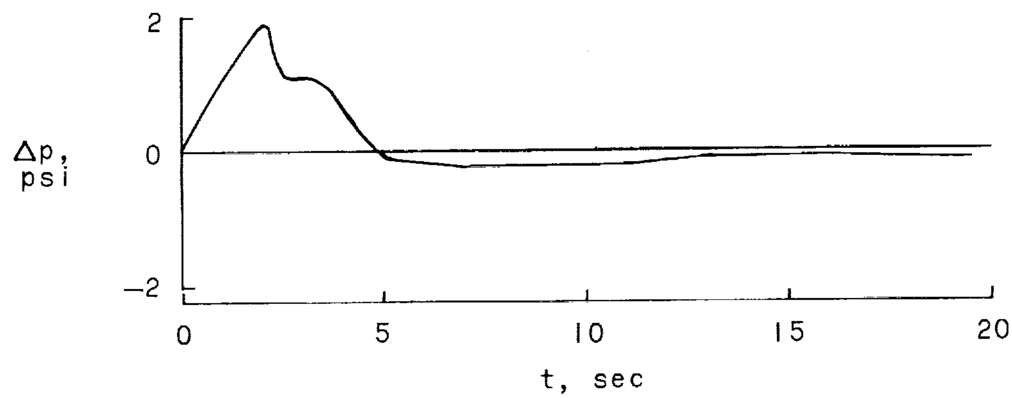

(a) Variation of differential pressure with time.

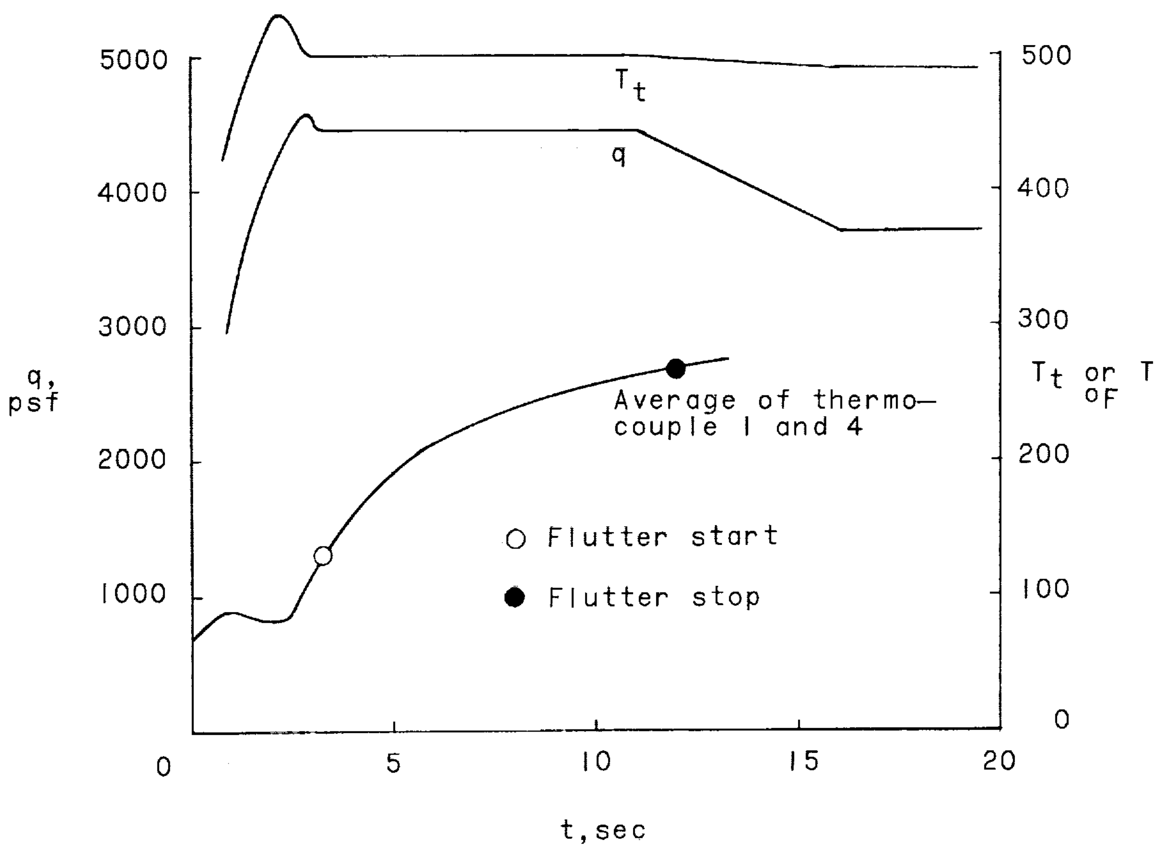

(b) Variation of dynamic pressure, stagnation temperature, and skin temperature with time.

Figure 9.- Test conditions of two-bay aluminum-alloy panel with film cooling during tunnel start. (Test 6.)

L-1630

L-1630

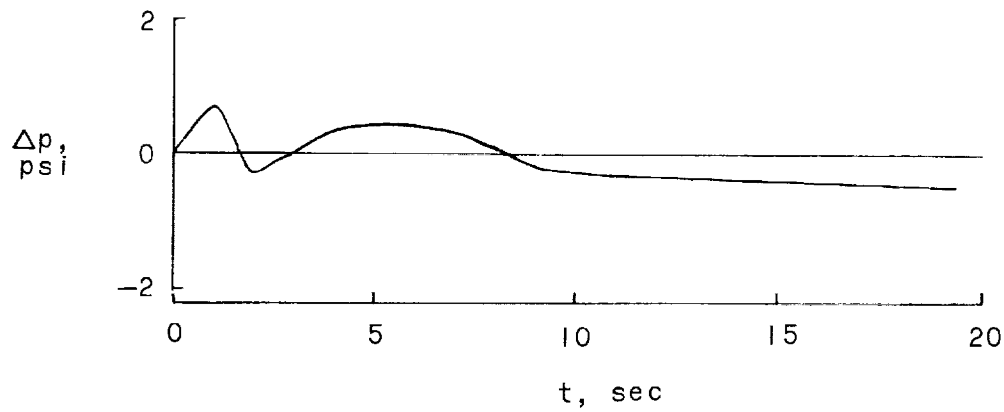

(a) Variation of differential pressure with time.

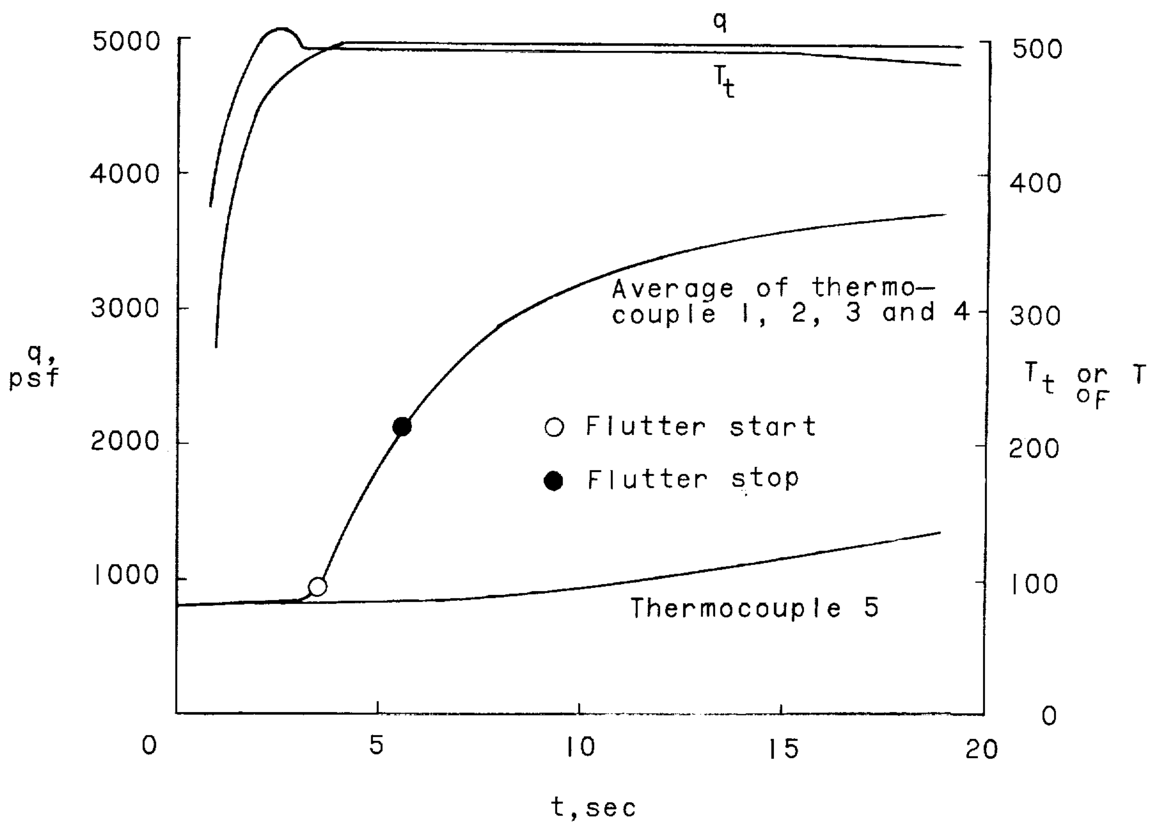

(b) Variation of dynamic pressure, stagnation temperature, and skin temperature with time.

Figure 10.- Test conditions of a four-bay steel panel with protective doors operating. (Test 6.)

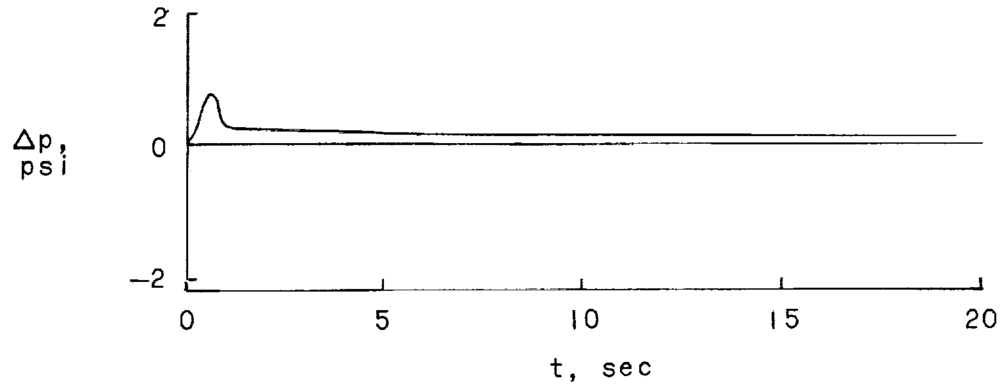

(a) Variation of differential pressure with time.

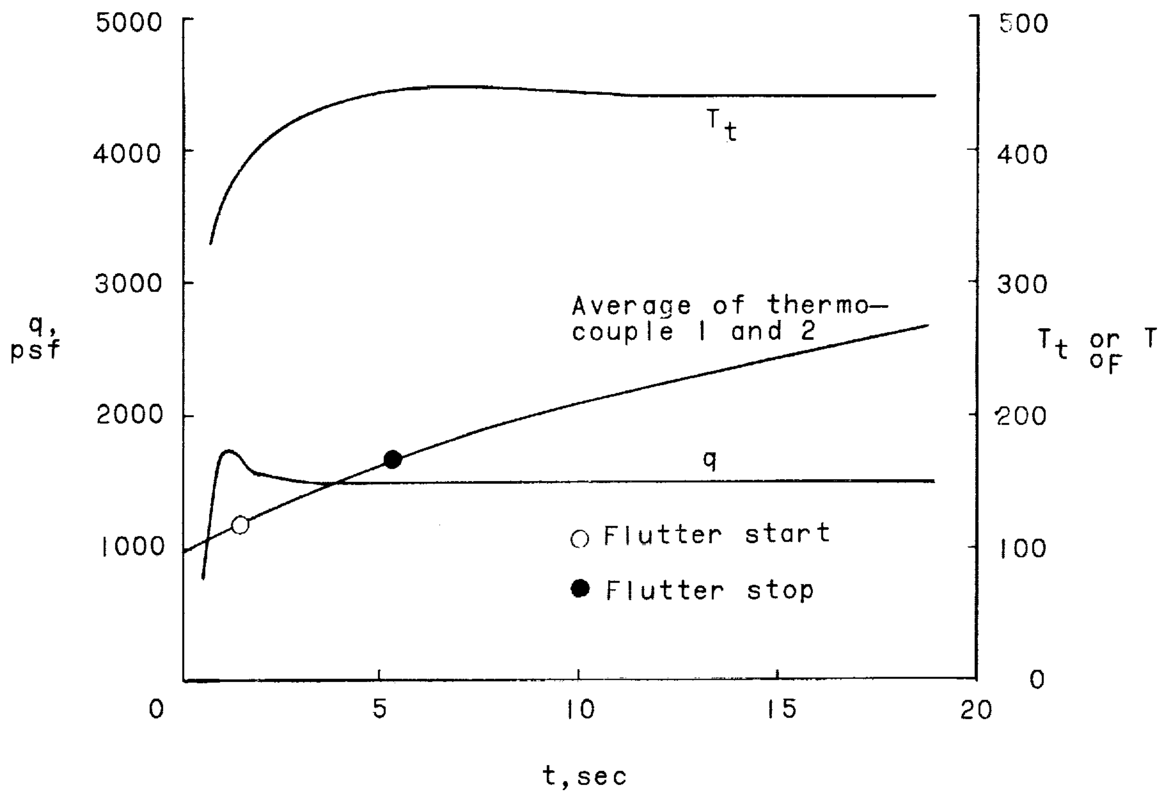

(b) Variation of dynamic pressure, stagnation temperature, and skin temperature with time.

Figure 11.- Typical test conditions of the X-15 lower vertical stabilizer. (Test 1.)

L-1630

(a) Start of flutter (panel flat).

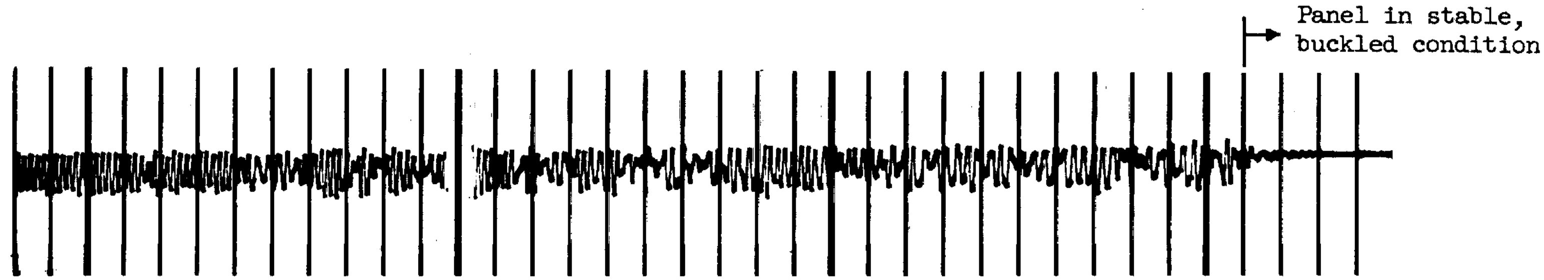

(b) Abrupt change in frequency. Erratic flutter.

Figure 12.- Sample deflectometer record for aluminum-alloy skin.

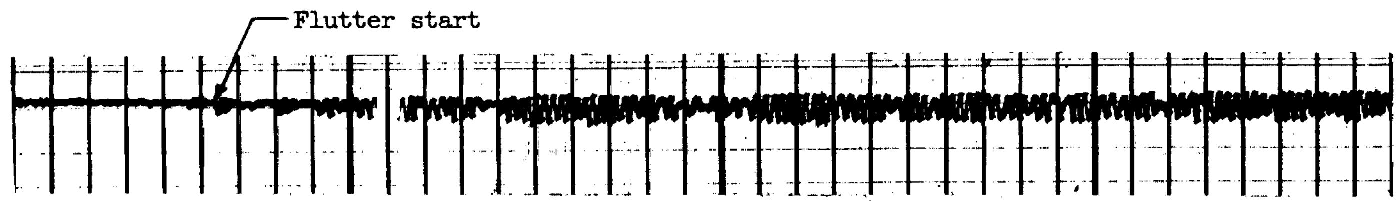

(a) Start of flutter (panel flat).

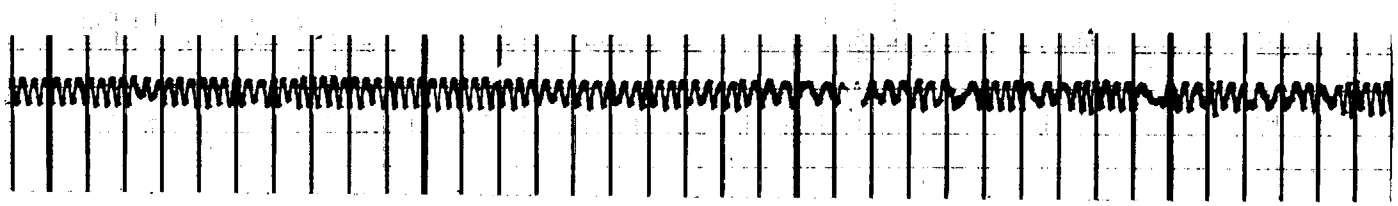

(b) Abrupt change in frequency. Erratic flutter.

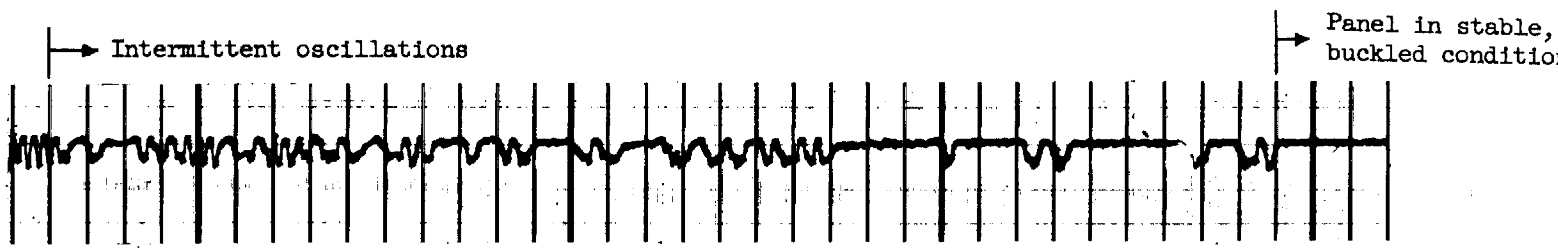

(c) Transition to intermittent oscillations.

Figure 13.- Sample deflectometer record for 17-7 PH stainless-steel skin.

L-1630

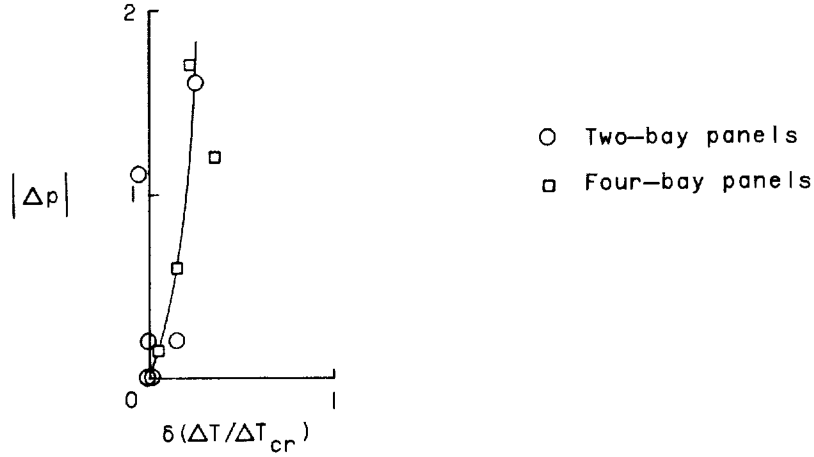

(a) Effect of pressure differential on temperature ratio.

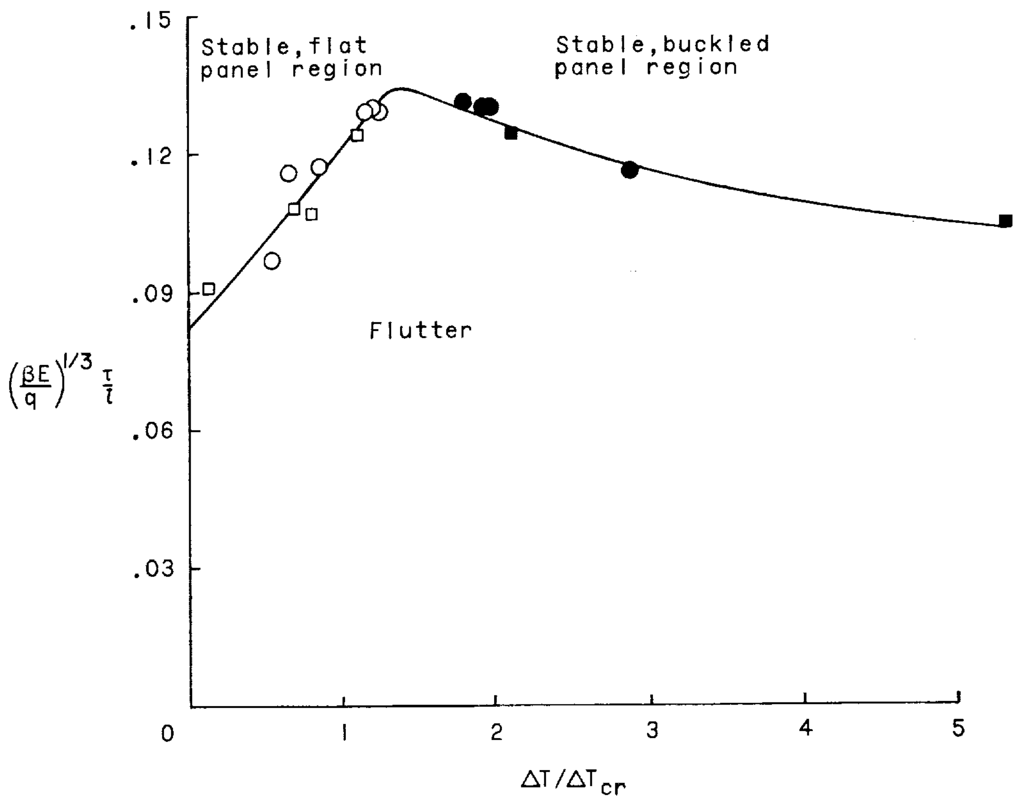

(b) Variation of modified-thickness-ratio parameter with temperature ratio.

Figure 14.- Flutter boundary for aluminum-alloy panels.

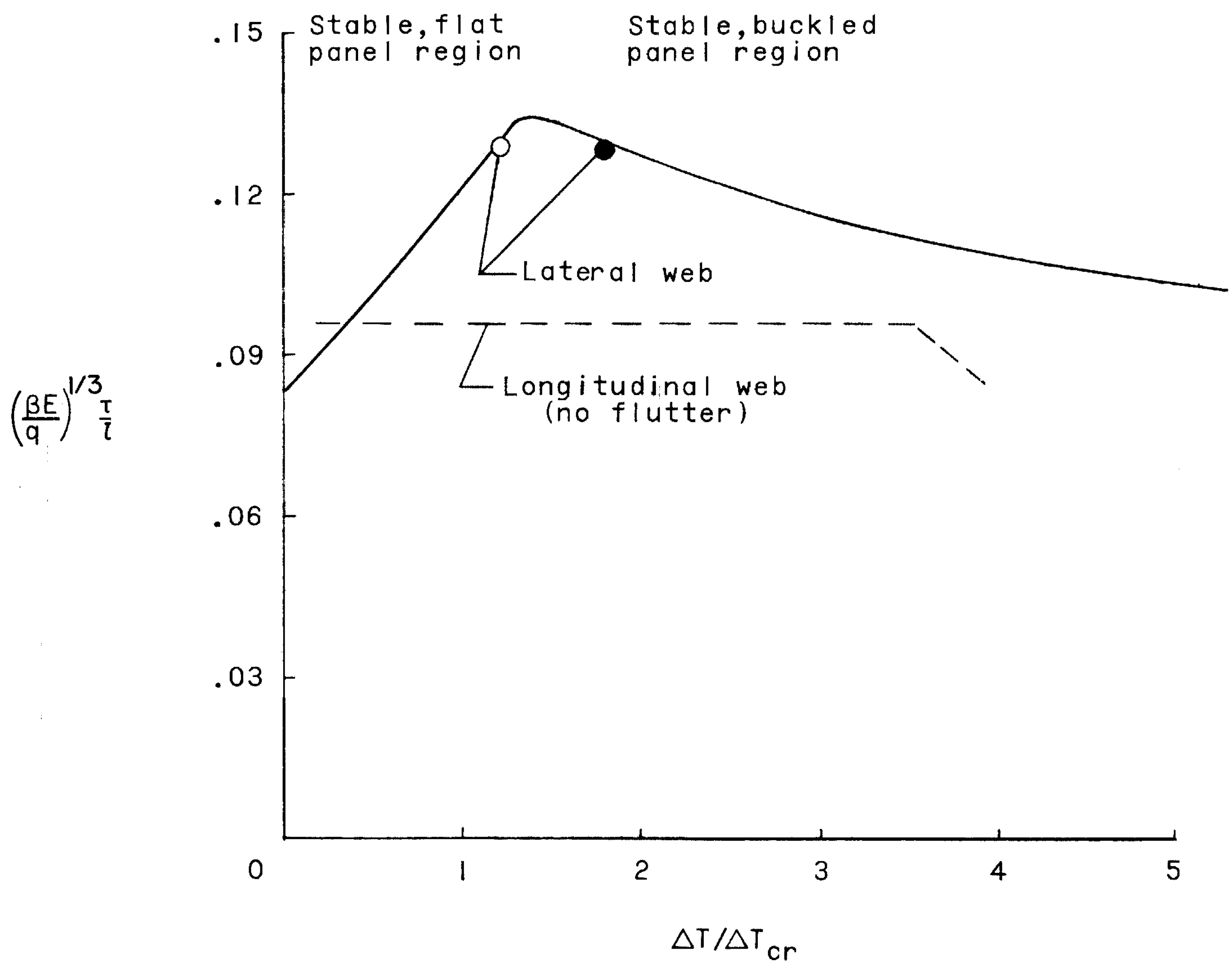

Figure 15.- Effect of lateral and longitudinal stiffeners on flutter of aluminum-alloy panels.

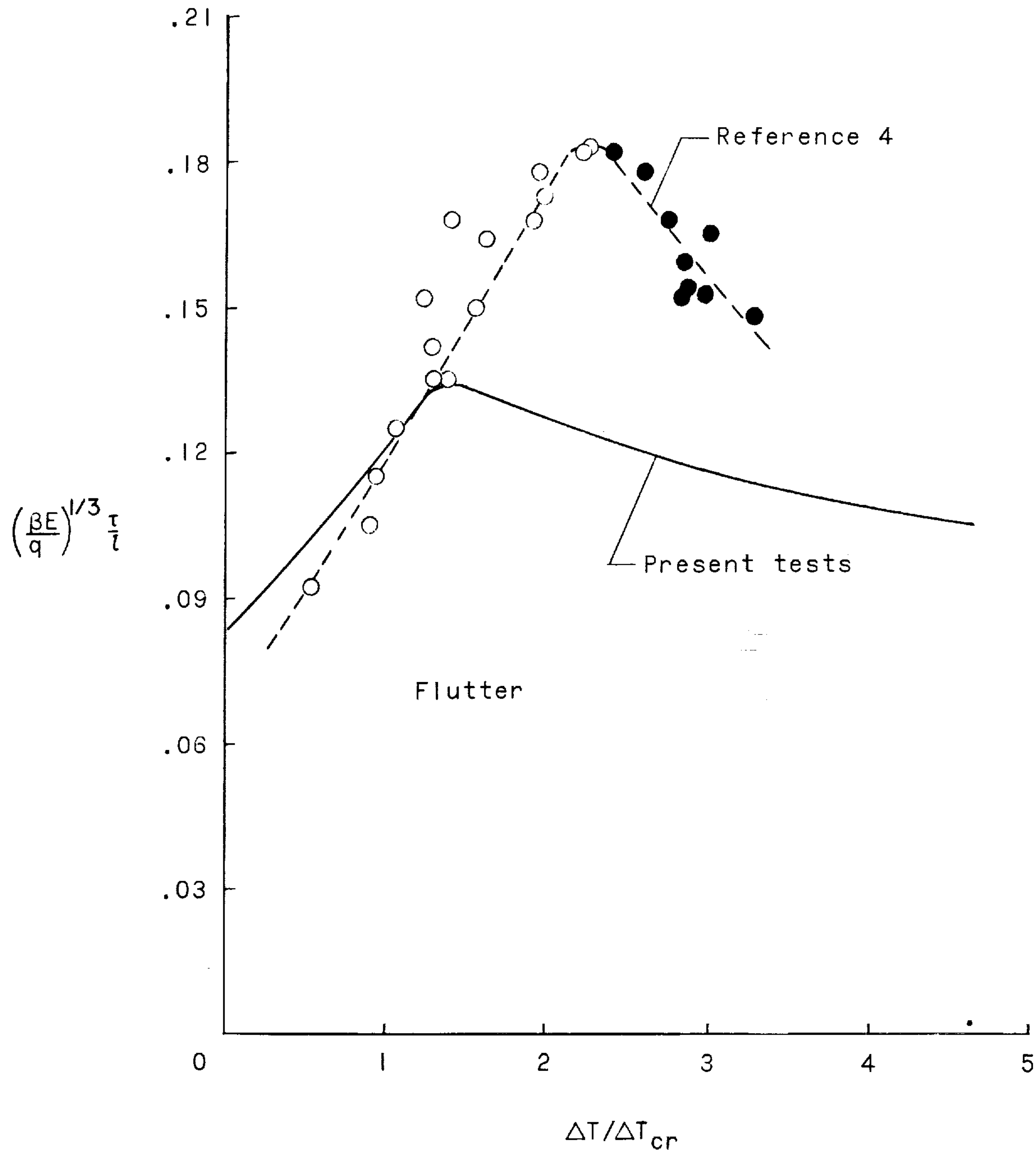

Figure 16.- Effect of end-support modification on flutter for aluminum-alloy panels.

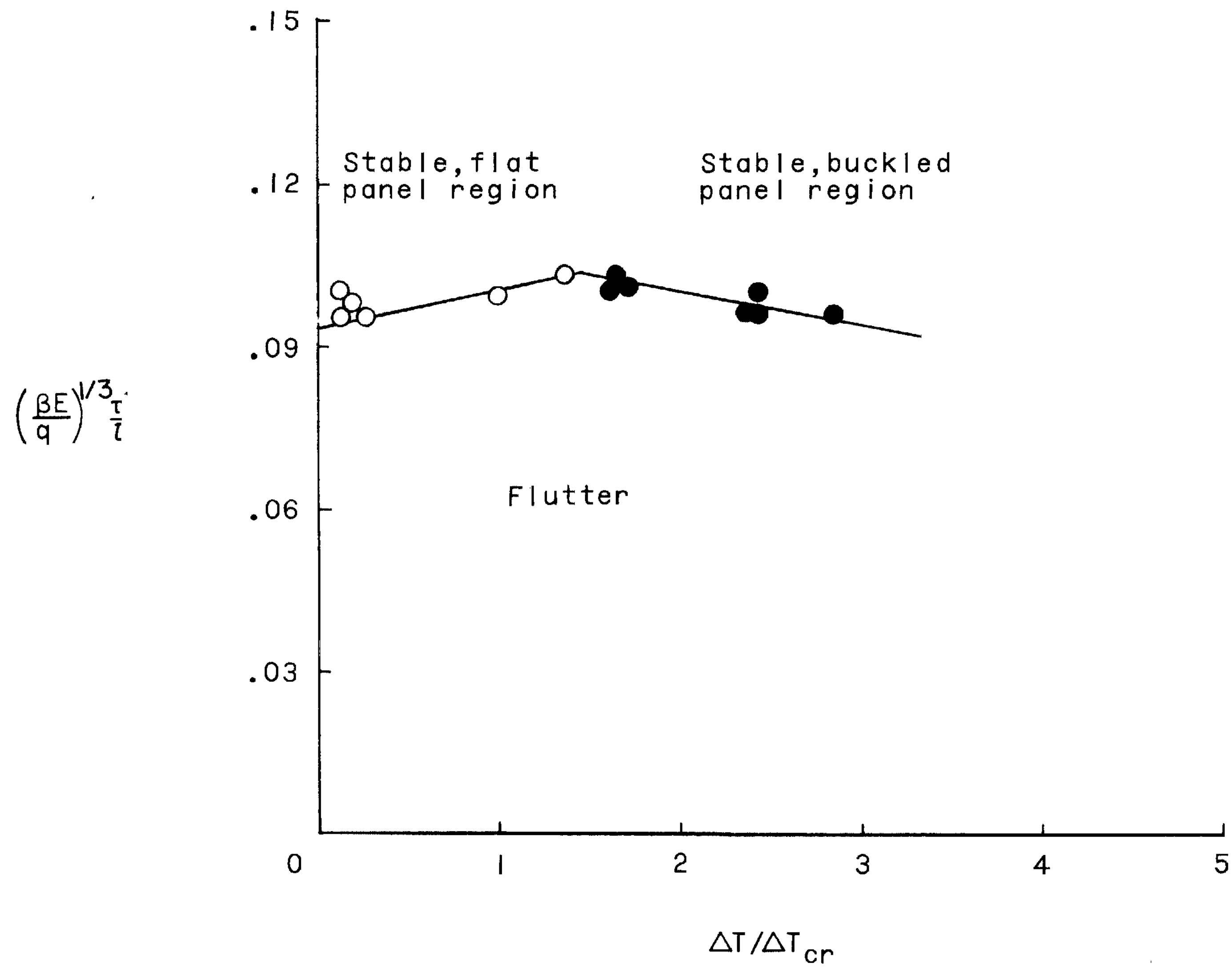

Figure 17.- Flutter boundary for 17-7 PH stainless-steel panels. Data are corrected for Δp.

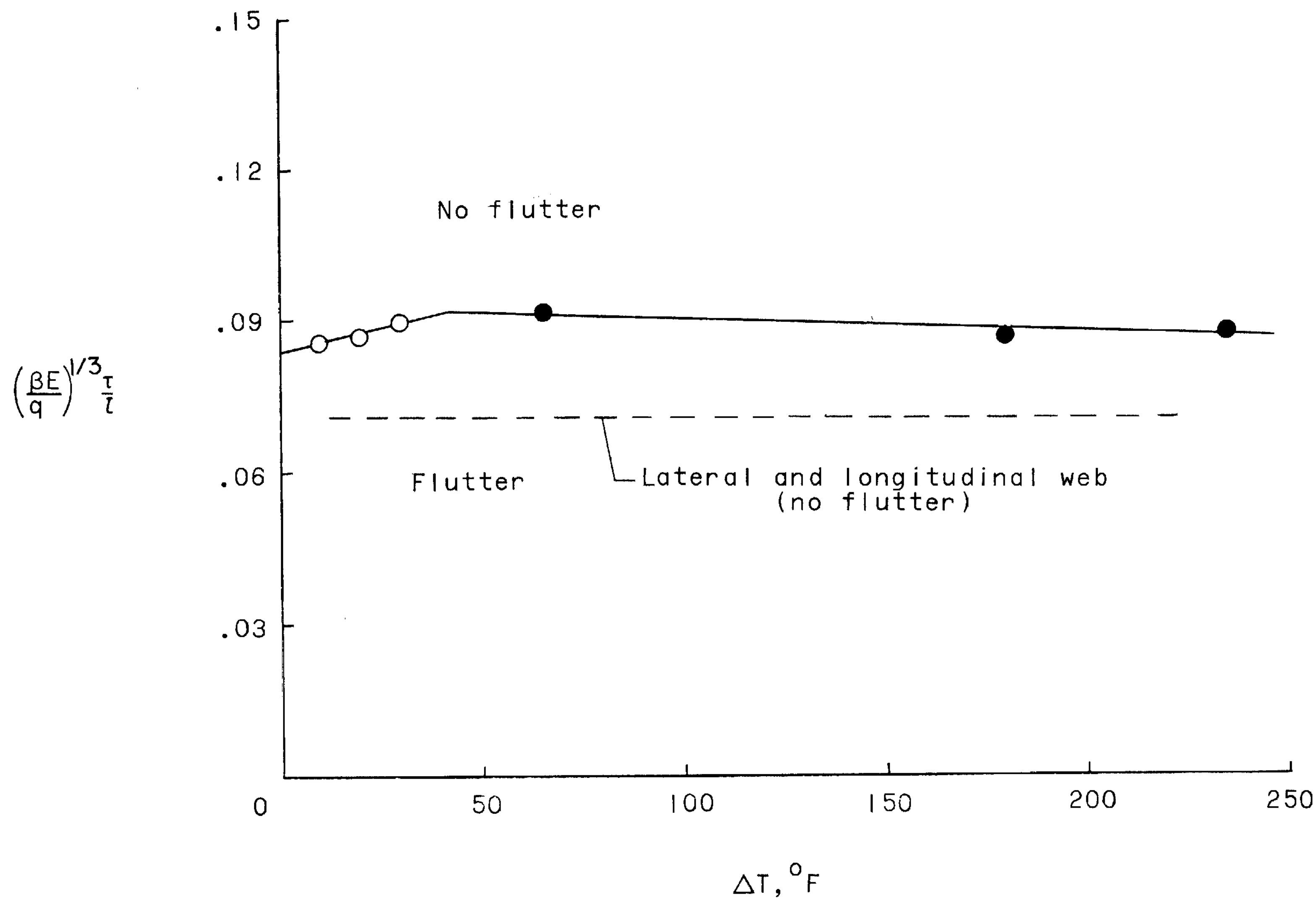

Figure 18.- Flutter boundary of X-15 vertical-stabilizer panels of length-width ratio of 10.

NASA-Langley, 1962 L-1630

NASA TN D-1353
National Aeronautics and Space Administration.
FLUTTER OF AERODYNAMICALLY HEATED ALUMINUM-ALLOY AND STAINLESS-STEEL PANELS WITH LENGTH-WIDTH RATIO OF 10 AT MACH NUMBER OF 3.0. Lawrence D. Guy and Herman L. Bohon. July 1962. 41p. OTS price, \$1.25. (NASA TECHNICAL NOTE D-1353)

Multibay panels were tested at dynamic pressures from 1,500 psf to 5,000 psf and at stagnation temperatures up to 660° F. Flutter boundaries were characterized by an increase in panel thickness required to prevent flutter with increasing thermally induced stress prior to buckling. After buckling the panels showed flutter boundaries characterized by a decrease in thickness required to prevent flutter with further increases in thermal stress. The largest thickness required to prevent flutter in the presence of aerodynamic heating occurred at the transition between the flat-panel boundary and buckled-panel boundary. The addition of a longitudinal stiffener in the center of a panel was effective in the prevention of flutter.

I. Guy, Lawrence D.
II. Bohon, Herman L.
III. NASA TN D-1353

(Initial NASA distribution: 51, Stresses and loads.)

NASA

NASA TN D-1353
National Aeronautics and Space Administration.
FLUTTER OF AERODYNAMICALLY HEATED ALUMINUM-ALLOY AND STAINLESS-STEEL PANELS WITH LENGTH-WIDTH RATIO OF 10 AT MACH NUMBER OF 3.0. Lawrence D. Guy and Herman L. Bohon. July 1962. 41p. OTS price, \$1.25. (NASA TECHNICAL NOTE D-1353)

Multibay panels were tested at dynamic pressures from 1,500 psf to 5,000 psf and at stagnation temperatures up to 660° F. Flutter boundaries were characterized by an increase in panel thickness required to prevent flutter with increasing thermally induced stress prior to buckling. After buckling the panels showed flutter boundaries characterized by a decrease in thickness required to prevent flutter with further increases in thermal stress. The largest thickness required to prevent flutter in the presence of aerodynamic heating occurred at the transition between the flat-panel boundary and buckled-panel boundary. The addition of a longitudinal stiffener in the center of a panel was effective in the prevention of flutter.

I. Guy, Lawrence D.
II. Bohon, Herman L.
III. NASA TN D-1353

(Initial NASA distribution: 51, Stresses and loads.)

NASA

NASA TN D-1353
National Aeronautics and Space Administration.
FLUTTER OF AERODYNAMICALLY HEATED ALUMINUM-ALLOY AND STAINLESS-STEEL PANELS WITH LENGTH-WIDTH RATIO OF 10 AT MACH NUMBER OF 3.0. Lawrence D. Guy and Herman L. Bohon. July 1962. 41p. OTS price, \$1.25. (NASA TECHNICAL NOTE D-1353)

Multibay panels were tested at dynamic pressures from 1,500 psf to 5,000 psf and at stagnation temperatures up to 660° F. Flutter boundaries were characterized by an increase in panel thickness required to prevent flutter with increasing thermally induced stress prior to buckling. After buckling the panels showed flutter boundaries characterized by a decrease in thickness required to prevent flutter with further increases in thermal stress. The largest thickness required to prevent flutter in the presence of aerodynamic heating occurred at the transition between the flat-panel boundary and buckled-panel boundary. The addition of a longitudinal stiffener in the center of a panel was effective in the prevention of flutter.

I. Guy, Lawrence D.
II. Bohon, Herman L.
III. NASA TN D-1353

(Initial NASA distribution: 51, Stresses and loads.)

NASA

NASA TN D-1353
National Aeronautics and Space Administration.
FLUTTER OF AERODYNAMICALLY HEATED ALUMINUM-ALLOY AND STAINLESS-STEEL PANELS WITH LENGTH-WIDTH RATIO OF 10 AT MACH NUMBER OF 3.0. Lawrence D. Guy and Herman L. Bohon. July 1962. 41p. OTS price, \$1.25. (NASA TECHNICAL NOTE D-1353)

Multibay panels were tested at dynamic pressures from 1,500 psf to 5,000 psf and at stagnation temperatures up to 660° F. Flutter boundaries were characterized by an increase in panel thickness required to prevent flutter with increasing thermally induced stress prior to buckling. After buckling the panels showed flutter boundaries characterized by a decrease in thickness required to prevent flutter with further increases in thermal stress. The largest thickness required to prevent flutter in the presence of aerodynamic heating occurred at the transition between the flat-panel boundary and buckled-panel boundary. The addition of a longitudinal stiffener in the center of a panel was effective in the prevention of flutter.

I. Guy, Lawrence D.
II. Bohon, Herman L.
III. NASA TN D-1353

(Initial NASA distribution: 51, Stresses and loads.)

NASA